Integral equations and related meshfree methods

Jan Sladek[a, *] and Vladimir Sladek[a]

[a] *Institute of Construction and Architecture, Slovak Academy of Sciences, 84503 Bratislava, Slovakia (*sladek@savba.sk)*

Aim to find efficient, power computational method to general boundary value problems.

Many problems are described by complicated governing equations and constitutive equations.

Coupled problems

Difference between the standard BEM and Local integral equations (LIE)

Elasticity

Governing equations

$$\sigma_{ij,j}(\mathbf{x},t) - \rho(\mathbf{x})\ddot{u}_i(\mathbf{x},t) = -X_i(\mathbf{x},t)\ . \qquad (1)$$

Constitutive equation

$$\sigma_{ij}(\mathbf{x},t) = C_{ijkl}(\mathbf{x})\varepsilon_{kl}(\mathbf{x},t) = C_{ijkl}(\mathbf{x})u_{k,l}(\mathbf{x},t)\ , \qquad (2)$$

The traction vector $t_i = \sigma_{ij} n_j$

$$t_i(\mathbf{x},t) = C_{ijkl}(\mathbf{x})u_{k,l}(\mathbf{x},t)n_j(\mathbf{x})\ \ . \qquad (3)$$

The weak-form of the governing equations (1)

Conventional BEM

$$\int_{\Omega} \left[\sigma_{ij,j}(\mathbf{x},\tau) - \rho(\mathbf{x})\ddot{u}_i(\mathbf{x},\tau) + X_i(\mathbf{x},\tau) \right] u_i^*(\mathbf{x})\, d\Omega = 0 \,, \qquad (4)$$

where $u_i^*(\mathbf{x})$ is a test function. Ω is global domain.

Substituting constitutive eq. (2) into the weak form

$$\int_{\Omega} \left[L_{ik} u_k(\mathbf{x},\tau) - \rho(\mathbf{x})\ddot{u}_i(\mathbf{x},\tau) + X_i(\mathbf{x},\tau) \right] u_i^*(\mathbf{x})\, d\Omega = 0, \qquad (5)$$

where operator $L_{ik} = C_{ijkl} \dfrac{\partial^2}{\partial x_j \partial x_l}$.

Lets $X_i = 0$ and 2x Gauss divergence to (5) – Somigliana identity

$$u_i(y,\tau) = \int_{\Gamma} \left[t_k(x,\tau) U_{ik}^*(x,y) - u_k(x,\tau) T_{ik}^*(x,y) \right] d\Gamma - \int_{\Omega} \rho \ddot{u}_k(x,\tau) U_{ik}^*(x,y) d\Omega$$

where

$$L_{ij} U_{jk}^*(x,y) = -\delta_{ik}\delta(x-y).$$

One can write

$$T^*_{ik} = c_{ijpl} n_j U_{pk,l} \quad \text{since} \quad t_i = \sigma_{ij} n_j = c_{ijpl} u_{p,l} n_j$$

Regularization

Applying Guass divergence to

$$\int_\Gamma T^*_{ik}(x,y)d\Gamma = \int_\Gamma c_{ijpl} n_j U^*_{pk,l}(x,y)d\Gamma = \int_\Omega c_{ijpl} U^*_{pk,lj}(x,y)d\Omega$$

where

$$c_{ijpl} U^*_{pk,lj} = -\delta_{ik}\delta(x-y)$$

Then,

$$\int_\Gamma T^*_{ik}(x,y)d\Gamma = \begin{cases} -\delta_{ik} & for \;\; y \in \Omega \\ 0 & for \;\; y \notin \Omega \end{cases} .$$

From Somigliana identity $u_i(y) = \delta_{ik} u_k(y)$

$$-\int_{\Gamma} u_k(y,\tau)T^*_{ik}(x,y)d\Gamma =$$

$$= \int_{\Gamma}\left[t_k(x,\tau)U^*_{ik}(x,y) - u_k(x,\tau)T^*_{ik}(x,y)\right]d\Gamma - \int_{\Omega}\rho\ddot{u}_k(x,\tau)U^*_{ik}(x,y)d\Omega \qquad (6)$$

Rearranging

$$\int_{\Gamma} T^*_{ik}(x,y)\left[u_k(x,\tau) - u_k(y,\tau)\right]d\Gamma - \int_{\Gamma} t_k(x,\tau)U^*_{ik}(x,y)d\Omega =$$

$$= -\int_{\Omega}\rho\ddot{u}_k(x,\tau)U^*_{ik}(x,y)d\Omega. \qquad (7)$$

Holder continuity $\left|u(y)-u(x)\right| \le A\left|y-x\right|^{\alpha}$

Local integral equations

Zhu, T., Zhang, J.D., Atluri, S.N. (1998): A local boundary integral equation (LBIE) method in computational mechanics, and a meshless discretization approaches. *Computational Mechanics*, 21, pp. 223-235.

Weak form on local subdomains

$$\int_{\Omega_s} \left[\sigma_{ij,j}(\mathbf{x},\tau) - \rho(\mathbf{x})\ddot{u}_i(\mathbf{x},\tau) + X_i(\mathbf{x},\tau) \right] u_i^*(\mathbf{x})\, d\Omega = 0. \tag{8}$$

applying the Gauss divergence theorem, 1x

$$\int_{\partial\Omega_s} \sigma_{ij}(\mathbf{x},\tau) n_j(\mathbf{x}) u_{ik}^*(\mathbf{x}) d\Gamma - \int_{\Omega_s} \sigma_{ij}(\mathbf{x},\tau) u_{ik,j}^*(\mathbf{x}) d\Omega +$$

$$- \int_{\Omega_s} \left[\rho(\mathbf{x})\ddot{u}_i(\mathbf{x},\tau) \right] u_{ik}^*(\mathbf{x}) d\Omega = 0. \tag{9}$$

If a Heaviside or unit step function is chosen as the test function

$$u_{ik}^*(\mathbf{x}) = \begin{cases} \delta_{ik} & \text{at} \quad \mathbf{x} \in \Omega_s \\ 0 & \text{at} \quad \mathbf{x} \notin \Omega_s \end{cases}$$

the local weak-form (9) is converted into the LIE

$$\int_{L_s+\Gamma_{su}} t_i(\mathbf{x},\tau)d\Gamma - \int_{\Omega_s} \rho\ddot{u}_i(\mathbf{x},\tau)d\Omega = -\int_{\Gamma_{st}} \tilde{t}_i(\mathbf{x},\tau)d\Gamma - \int_{\Omega_s} X_i(\mathbf{x},\tau)d\Omega\,. \qquad (10)$$

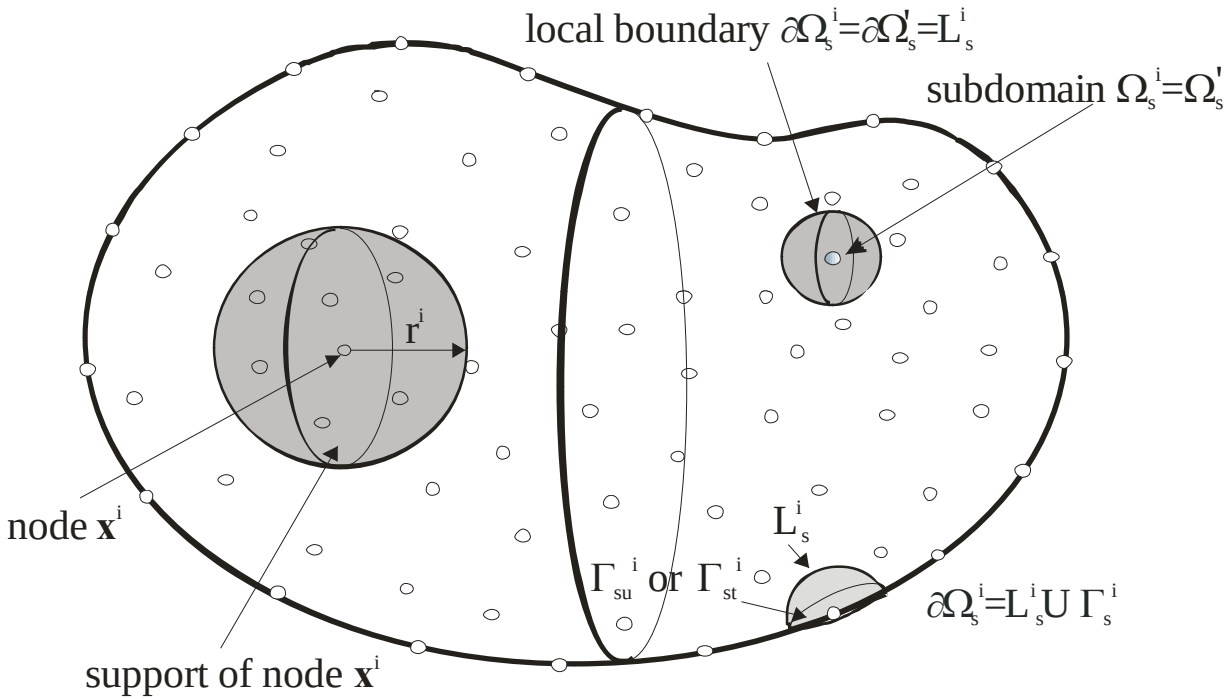

Fig. 1 Local boundaries for weak-form formulation and support domain of weight function at node $\mathbf{x}^i$

Local integral equation is related to one node
Therefore, approximation has to be global

Numerical solution

Belytschko T, Krogauz Y, Organ D, Fleming M, Krysl P (1996) Meshless methods; an overview and recent developments. Comp. Meth. Appl. Mech. Engn. 139: 3-47.

The trial function is chosen to be the moving least-squares (MLS) approximation over a number of nodes randomly spread within the domain of influence.

The MLS approximant $\mathbf{u}^h(\mathbf{x},\tau)$ of $\mathbf{u}$ is defined by

$$\mathbf{u}^h(\mathbf{x},\tau) = \mathbf{p}^T(\mathbf{x})\mathbf{a}(\mathbf{x},\tau)\ . \tag{11}$$

The complete monomial basis of order *m*; for example, in 2-D problems

$\mathbf{p}^T(\mathbf{x}) = \{1, x_1, x_2\}$ for m=3

and

$\mathbf{p}^T(\mathbf{x}) = \{1, x_1, x_2, x_1^2, x_1x_2, x_2^2\}$ for m=6 (12)

are linear and quadratic basis functions, respectively.

In 3-D problems, the linear basis is defined as

$$\mathbf{p}^T(\mathbf{x}) = \left[1,\ x_1,\ x_2, x_3\right] ,$$

and the quadratic basis is defined as

$$\mathbf{p}^T(\mathbf{x}) = \left[1,\ x_1,\ x_2,\ x_3, x_1^2,\ x_2^2, x_3^2, x_1x_2, x_1x_3, x_3x_2\right] \quad .$$

The coefficient vector $\mathbf{a}(\mathbf{x})$ is determined by minimizing a weighted discrete L_2 -norm defined as

$$J(\mathbf{x}) = \sum_{a=1}^{n} w^a(\mathbf{x})\left[\mathbf{p}^T(\mathbf{x}^a)\mathbf{a}(\mathbf{x},\tau) - \hat{\mathbf{u}}^a(\tau)\right]^2 \quad . \tag{13}$$

Final approximation formula

$$\mathbf{u}^h(\mathbf{x},\tau) = \mathbf{\Phi}^T(\mathbf{x})\cdot\hat{\mathbf{u}}(\tau) = \sum_{a=1}^{n}\phi^a(\mathbf{x})\hat{\mathbf{u}}^a(\tau) \quad , \tag{14}$$

A 4th-order spline-type weight function is applied in the present work

$$w^a(\mathbf{x}) = \begin{cases} 1 - 6\left(\dfrac{d^a}{r^a}\right)^2 + 8\left(\dfrac{d^a}{r^a}\right)^3 - 3\left(\dfrac{d^a}{r^a}\right)^4 & 0 \le d^a \le r^a \\ 0 & d^a \ge r^a \end{cases} ,$$

The traction vector

$$\mathbf{t}^h(\mathbf{x},\tau) = \mathbf{N}(\mathbf{x})\mathbf{C}\sum_{a=1}^{n}\mathbf{B}^a(\mathbf{x})\hat{\mathbf{u}}^a(\tau) \quad , \qquad (15)$$

where the matrix **N(x)** is related to the normal vector **n(x)**

$$\mathbf{N}(\mathbf{x}) = \begin{bmatrix} n_1 & 0 & 0 & 0 & n_3 & n_2 \\ 0 & n_2 & 0 & n_3 & 0 & n_1 \\ 0 & 0 & n_3 & n_2 & n_1 & 0 \end{bmatrix} \qquad \text{for 3-D}$$

and $\mathbf{N}(\mathbf{x}) = \begin{bmatrix} n_1 & 0 & n_2 \\ 0 & n_2 & n_1 \end{bmatrix}$ for 2-D problems.

The matrix $\mathbf{B}^a$ is represented by the gradients of the shape functions for 3-D as

$$\mathbf{B}^a = \begin{bmatrix} \phi^a_{,1} & 0 & 0 \\ 0 & \phi^a_{,2} & 0 \\ 0 & 0 & \phi^a_{,3} \\ 0 & \phi^a_{,3} & \phi^a_{,2} \\ \phi^a_{,3} & 0 & \phi^a_{,1} \\ \phi^a_{,2} & \phi^a_{,1} & 0 \end{bmatrix} \quad \text{and} \quad \mathbf{B}^a(\mathbf{x}) = \begin{bmatrix} \phi^a_{,1} & 0 \\ 0 & \phi^a_{,2} \\ \phi^a_{,2} & \phi^a_{,1} \end{bmatrix} \text{ for 2-D problems.}$$

Substituting the MLS approximations into LIEs (10) for each of the internal nodes $\mathbf{x}^i$, the following set of discretized LIEs is obtained

$$\sum_{a=1}^{n} \left[\left(\int_{L_s^i} \mathbf{N}(\mathbf{x}) \mathbf{C} \mathbf{B}^a(\mathbf{x}) d\Gamma \right) \hat{\mathbf{u}}^a(\tau) - \rho \left(\int_{\Omega_s^i} \phi^a(\mathbf{x}) d\Omega \right) \ddot{\hat{\mathbf{u}}}^a(\tau) \right] - = -\int_{\Omega_s^i} \mathbf{X}(\mathbf{x}, \tau) d\Omega. \qquad (16)$$

The system of ODE can be rearranged in such a way that all known quantities are on the r.h.s. Thus, in matrix form the system becomes

$$\mathbf{A}\ddot{\mathbf{x}} + \mathbf{C}\mathbf{x} = \mathbf{Y} \quad . \tag{17}$$

The Houbolt finite- difference scheme

$$\ddot{\mathbf{x}}_{\tau+\Delta\tau} = \frac{2\mathbf{x}_{\tau+\Delta\tau} - 5\mathbf{x}_{\tau} + 4\mathbf{x}_{\tau-\Delta\tau} - \mathbf{x}_{\tau-2\Delta\tau}}{\Delta\tau^2} \quad ,$$

where $\Delta\tau$ is the time step.

The system of algebraic equations for the unknowns $\mathbf{x}_{\tau+\Delta\tau}$

$$\left[\frac{2}{\Delta\tau^2}\mathbf{A} + \mathbf{C}\right]\mathbf{x}_{\tau+\Delta\tau} = \frac{1}{\Delta\tau^2}5\mathbf{A}\mathbf{x}_{\tau} + \\ + \mathbf{A}\frac{1}{\Delta\tau^2}\left\{-4\mathbf{x}_{\tau-\Delta\tau} + \mathbf{x}_{\tau-2\Delta\tau}\right\} + \mathbf{Y}. \tag{18}$$

Numerical example

material properties for a homogeneous orthotropic strip: $E_1 = 2 \cdot 10^4$, $E_2 = 10^4$, $G_{12} = 0.416 \cdot 10^4$, $\nu_{12} = 0.2$ and $\rho = 1$.

FGM orthotropic strip, only $E_1 = E_{10} \exp(\gamma x_1)$, while other material parameters are considered to be uniform.

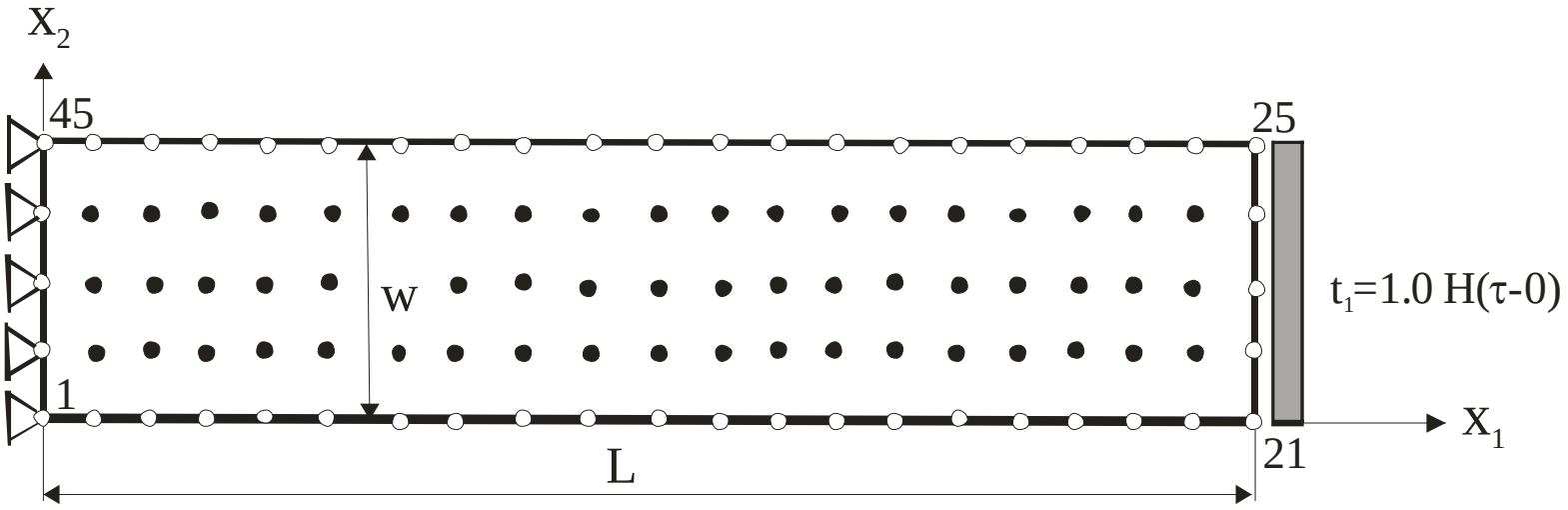

Fig. 2 An orthotropic FGM strip under a uniaxial tension

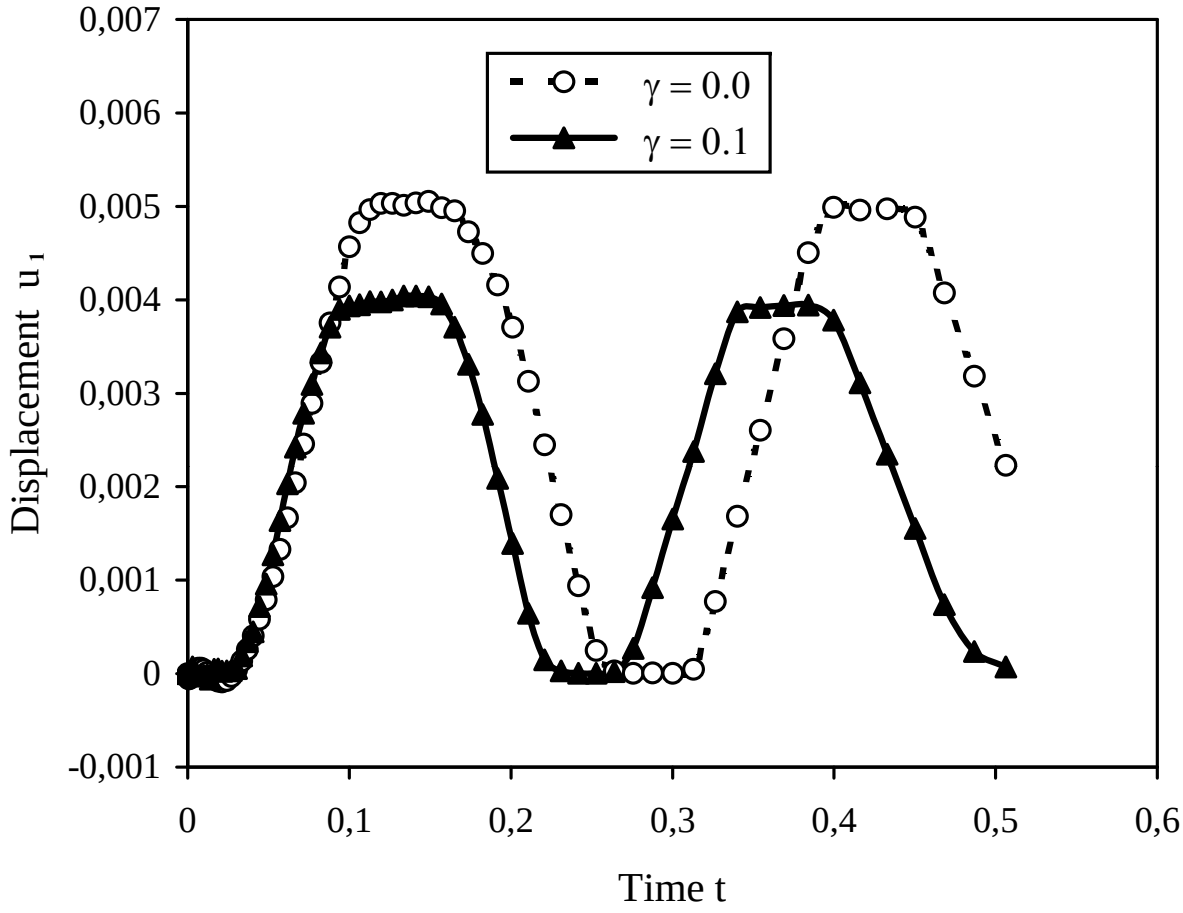

Fig. 3 Influence of the gradient parameter on the time variation of the displacement component in an orthotropic FGM strip

Modern technologies require new **sophisticated materials.**

In advanced materials new phenomena are observed, like coupling of physical fields.

In thermoelasticity thermal effects can include heat production due to the strain rate, i.e. the thermoelastic dissipation.

Modern smart structures made of piezoelectric and piezomagnetic materials offer certain potential performance advantages over conventional ones due to their capability of converting the energy from one type to other (among magnetic, electric, and mechanical).

The local integral equation method in transient coupled thermoelasticity

The equilibrium and the thermal balance equations in transient coupled thermoelasticity [Nowacki (1986)] can be written as

$$\sigma_{ij,j}(\mathbf{x},\tau)-\rho\ddot{u}_i(\mathbf{x},\tau)+X_i(\mathbf{x},\tau)=0, \tag{1}$$

$$\left[k_{ij}(\mathbf{x})\theta_{,j}(\mathbf{x},\tau)\right]_{,i}-\rho c\dot{\theta}(\mathbf{x},\tau)-\gamma_{ij}\theta_0\dot{u}_{i,j}(\mathbf{x},\tau)+Q(\mathbf{x},\tau)=0\,, \tag{2}$$

Duhamel-Neumann constitutive equation for the stress tensor

$$\sigma_{ij}(\mathbf{x},\tau)=c_{ijkl}\varepsilon_{kl}(\mathbf{x},\tau)-\gamma_{ij}\theta(\mathbf{x},\tau), \tag{3}$$

Instead of writing the global weak-form for the above governing equations, the MLPG method constructs a weak-form over the local fictitious subdomains such as Ω_s, [Atluri (2004)]

$$\int_{\Omega_s} \left[\sigma_{ij,j}(\mathbf{x},\tau) - \rho \ddot{u}_i(\mathbf{x},\tau) + X_i(\mathbf{x},\tau) \right] u^*_{ik}(\mathbf{x})\, d\Omega \;\; = 0, \qquad (4)$$

By choosing a Heaviside step function as the test function

$$u^*_{ik}(\mathbf{x}) = \begin{cases} \delta_{ik} & \text{at} \quad \mathbf{x} \in \Omega_s \\ 0 & \text{at} \quad \mathbf{x} \notin \Omega_s \end{cases},$$

the local weak-form (4) is converted into the LIE

$$\int_{L_s + \Gamma_{su}} t_i(\mathbf{x},\tau) d\Gamma - \int_{\Omega_s} \rho \ddot{u}_i(\mathbf{x},\tau) d\Omega = - \int_{\Gamma_{st}} \tilde{t}_i(\mathbf{x},\tau) d\Gamma - \int_{\Omega_s} X_i(\mathbf{x},\tau) d\Omega \,. \qquad (5)$$

Non-homogeneous material properties are included in eq. (5) through the elastic and thermo-elastic coefficients

$$t_i(\mathbf{x},\tau) = \left[c_{ijkl}(\mathbf{x}) u_{k,l}(\mathbf{x},\tau) - \lambda_{ij}(\mathbf{x}) \theta(\mathbf{x},\tau) \right] n_j(\mathbf{x}).$$

Similarly, the local weak-form of the governing equation (2)

$$\int_{\Omega_s} \left\{ \left[k_{ij}(\mathbf{x}) \theta_{,j}(\mathbf{x},\tau) \right]_{,i} - \rho c \dot{\theta}(\mathbf{x},\tau) - \gamma_{ij} \theta_0 \dot{u}_{i,j}(\mathbf{x},\tau) + Q(\mathbf{x},\tau) \right\} u^*(\mathbf{x}) \, d\Omega = 0.$$

Applying the Gauss divergence theorem to the local weak-form and considering the Heaviside step function for the test function

$$\int_{L_s + \Gamma_{sp}} q(\mathbf{x},\tau) d\Gamma - \int_{\Omega_s} \rho c \dot{\theta}(x,\tau) d\Omega - \int_{\Omega_s} \gamma_{ij} \theta_0 \dot{u}_{i,j}(\mathbf{x},\tau) d\Omega =$$

$$= - \int_{\Gamma_{sq}} \tilde{q}(\mathbf{x},\tau) d\Gamma - \int_{\Omega_s} Q(\mathbf{x},\tau) d\Omega. \qquad (6)$$

Numerical solution

$$\mathbf{u}^h(\mathbf{x},\tau) = \mathbf{\Phi}^T(\mathbf{x}) \cdot \hat{\mathbf{u}}(\tau) = \sum_{a=1}^{n} \phi^a(\mathbf{x}) \hat{\mathbf{u}}^a(\tau) \quad , \qquad (7)$$

$$\theta^h(\mathbf{x},\tau) = \sum_{a=1}^{n} \phi^a(\mathbf{x}) \hat{\theta}^a(\tau) \quad .$$

The traction vector

$$\mathbf{t}^h(\mathbf{x},\tau)=\mathbf{N}(\mathbf{x})\mathbf{C}\sum_{a=1}^{n}\mathbf{B}^a(\mathbf{x})\hat{\mathbf{u}}^a(\tau)-\mathbf{N}(\mathbf{x})\boldsymbol{\gamma}\sum_{a=1}^{n}\phi^a(\mathbf{x})\hat{\theta}^a(\tau)\ \ , \tag{8}$$

Similarly the heat flux $q(\mathbf{x},\tau)$ can be approximated by

$$q^h(\mathbf{x},\tau)=k_{ij}n_i\sum_{a=1}^{n}\phi^a_{,j}(\mathbf{x})\hat{\theta}^a(\tau). \tag{9}$$

Substituting the MLS approximations into LIEs (5)and (6) for each of the internal nodes $\mathbf{x}^i$, the following set of discretized LIEs is obtained

$$\sum_{a=1}^{n}\left[\left(\int_{L_s^i}\mathbf{N}(\mathbf{x})\mathbf{C}\mathbf{B}^a(\mathbf{x})d\Gamma\right)\hat{\mathbf{u}}^a(\tau)-\rho\left(\int_{\Omega_s^i}\phi^a(\mathbf{x})d\Omega\right)\ddot{\hat{\mathbf{u}}}^a(\tau)\right]\ -$$

$$-\sum_{a=1}^{n}\left(\int_{L_s+\Gamma_{su}}\mathbf{N}(\mathbf{x})\boldsymbol{\gamma}\phi^a(\mathbf{x})d\Gamma\right)\hat{\theta}^a(\tau)\ =-\int_{\Omega_s^i}\mathbf{X}(\mathbf{x},\tau)d\Omega. \tag{10}$$

$$\sum_{a=1}^{n} \hat{\theta}^a(\tau) \int_{\partial\Omega_s^i} \mathbf{n}^T(\mathbf{x})\mathbf{K}(\mathbf{x})\mathbf{P}^a(\mathbf{x})d\Gamma - \sum_{a=1}^{n} \dot{\hat{\theta}}^a(\tau) \int_{\Omega_s^i} \rho c \phi^a(\mathbf{x})d\Omega -$$

$$-\sum_{a=1}^{n}\left(\int_{\Omega_s} \theta_0 \boldsymbol{\gamma}^T \mathbf{B}^a(\mathbf{x})d\Gamma \right) \dot{\hat{\mathbf{u}}}^a(\tau) = -\int_{\Gamma_{sq}} \tilde{q}(\mathbf{x},\tau)d\Gamma - \int_{\Omega_s} Q(\mathbf{x},\tau)d\Omega, \qquad (11)$$

where for 3-D problems

$$\mathbf{K}(\mathbf{x}) = \begin{bmatrix} k_{11} & k_{12} & k_{13} \\ k_{12} & k_{22} & k_{23} \\ k_{13} & k_{23} & k_{33} \end{bmatrix}, \qquad \mathbf{P}^a(\mathbf{x}) = \begin{bmatrix} \phi^a_{,1} \\ \phi^a_{,2} \\ \phi^a_{,3} \end{bmatrix}, \qquad \mathbf{n}^T = (n_1, n_2, n_3)$$

and for 2-D problems

$$\mathbf{K}(\mathbf{x}) = \begin{bmatrix} k_{11} & k_{12} \\ k_{12} & k_{22} \end{bmatrix}, \qquad \mathbf{P}^a(\mathbf{x}) = \begin{bmatrix} \phi^a_{,1} \\ \phi^a_{,2} \end{bmatrix}, \qquad \mathbf{n}^T = (n_1, n_2).$$

The system of ODE can be rearranged in such a way that all known quantities are on the r.h.s. Thus, in matrix form the system becomes

$$\mathbf{A}\ddot{\mathbf{x}} + \mathbf{B}\dot{\mathbf{x}} + \mathbf{C}\mathbf{x} = \mathbf{Y} \quad . \tag{12}$$

The Houbolt finite- difference scheme

$$\ddot{\mathbf{x}}_{\tau+\Delta\tau} = \frac{2\mathbf{x}_{\tau+\Delta\tau} - 5\mathbf{x}_{\tau} + 4\mathbf{x}_{\tau-\Delta\tau} - \mathbf{x}_{\tau-2\Delta\tau}}{\Delta\tau^2} \quad .$$

The backward difference method is applied for the approximation of "velocities"

$$\dot{\mathbf{x}}_{\tau+\Delta\tau} = \frac{\mathbf{x}_{\tau+\Delta\tau} - \mathbf{x}_{\tau}}{\Delta\tau} \quad .$$

The system of algebraic equations for the unknowns $\mathbf{x}_{\tau+\Delta\tau}$

$$\left[\frac{2}{\Delta\tau^2}\mathbf{A} + \frac{1}{\Delta\tau}\mathbf{B} + \mathbf{C}\right]\mathbf{x}_{\tau+\Delta\tau} = \frac{1}{\Delta\tau^2}(5\mathbf{A} + \mathbf{B}\Delta\tau)\mathbf{x}_{\tau} +$$

$$+\mathbf{A}\frac{1}{\Delta\tau^2}\left\{-4\mathbf{x}_{\tau-\Delta\tau} + \mathbf{x}_{\tau-2\Delta\tau}\right\} + \mathbf{Y}. \tag{13}$$

Numerical examples

3-D analysis of a clamped L-shaped console

The following parameters for a monoclinic material are used:

$$\mathbf{C} = \begin{bmatrix} 430.1 & 130.4 & 18.2 & 0 & 0 & 201.3 \\ 130.4 & 116.7 & 21 & 0 & 0 & 70.1 \\ 18.2 & 21 & 73.6 & 0 & 0 & 2.4 \\ 0 & 0 & 0 & 19.8 & -8 & 0 \\ 0 & 0 & 0 & -8 & 29.1 & 0 \\ 201.3 & 70.1 & 2.4 & 0 & 0 & 147.3 \end{bmatrix} GPa;$$

the stress-temperature coefficients

$$\boldsymbol{\gamma} = \begin{bmatrix} 1.01 & 2 & 0 \\ 2 & 1.48 & 0 \\ 0 & 0 & 7.52 \end{bmatrix} * 10^6 \, N / \deg m^2;$$

the mass density $\rho = 7820\,kg/m^3$, and the heat capacity $c = 461\,J/\deg kg$.

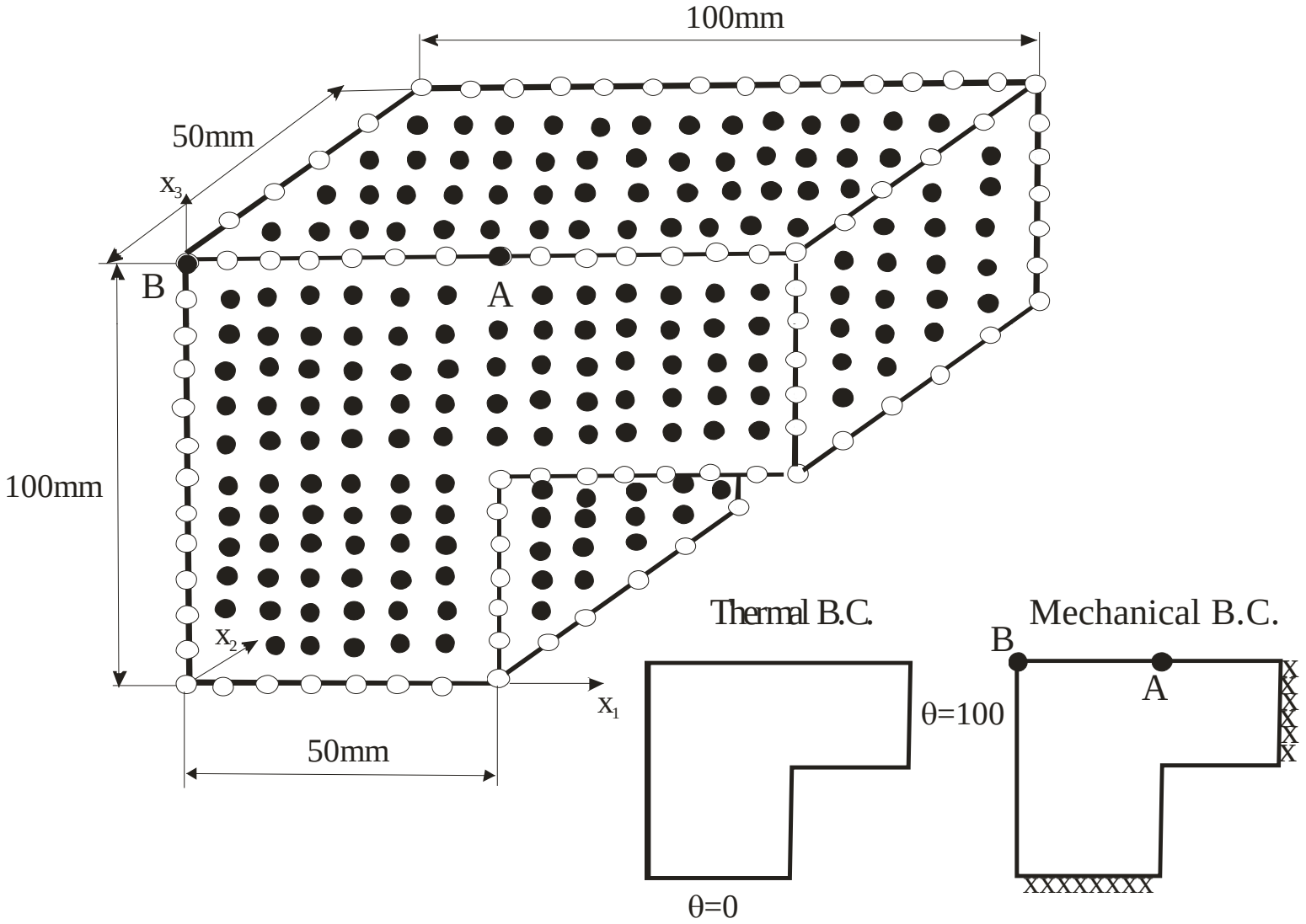

Fig. 2 Clamped L-shaped console under a thermal load

The total number of nodes is thus 6*341=2046.
Stationary boundary conditions in uncoupled thermoelasticity

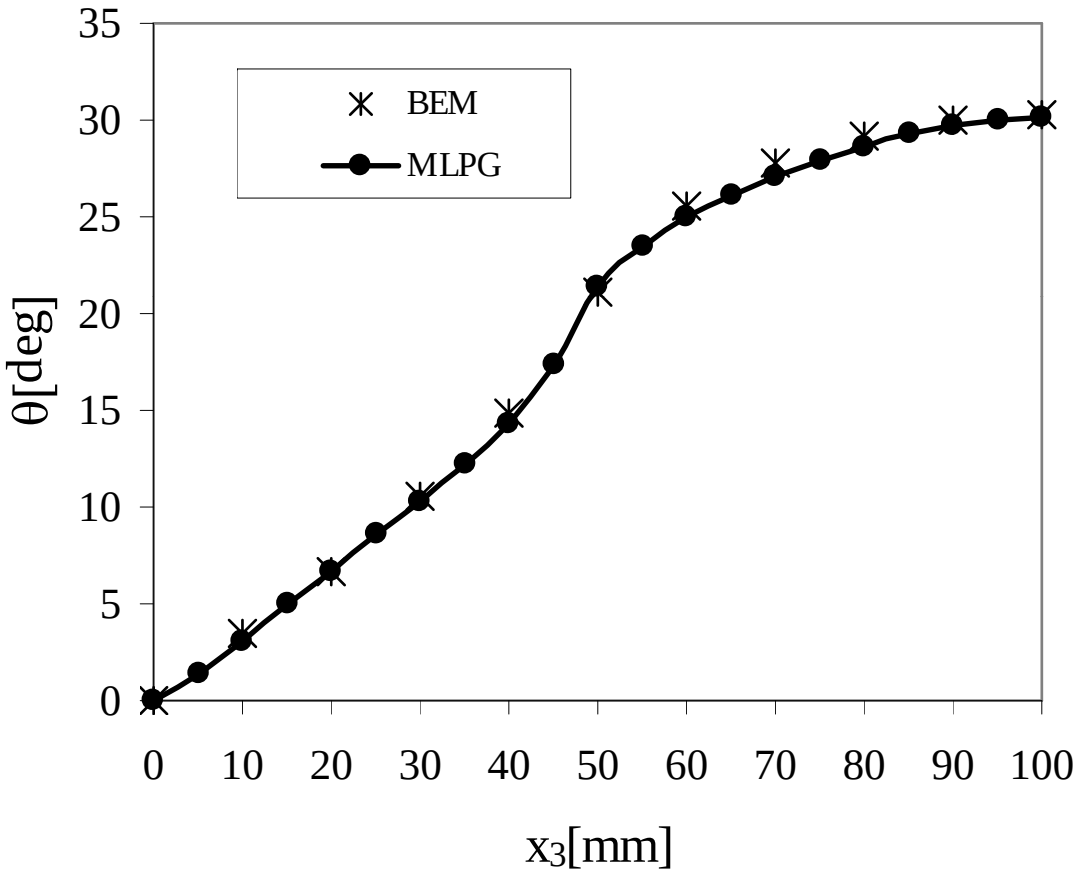

Fig. 3 Variation of the temperature along x_3.-axis at $x_1 = 50mm$ under stationary conditions

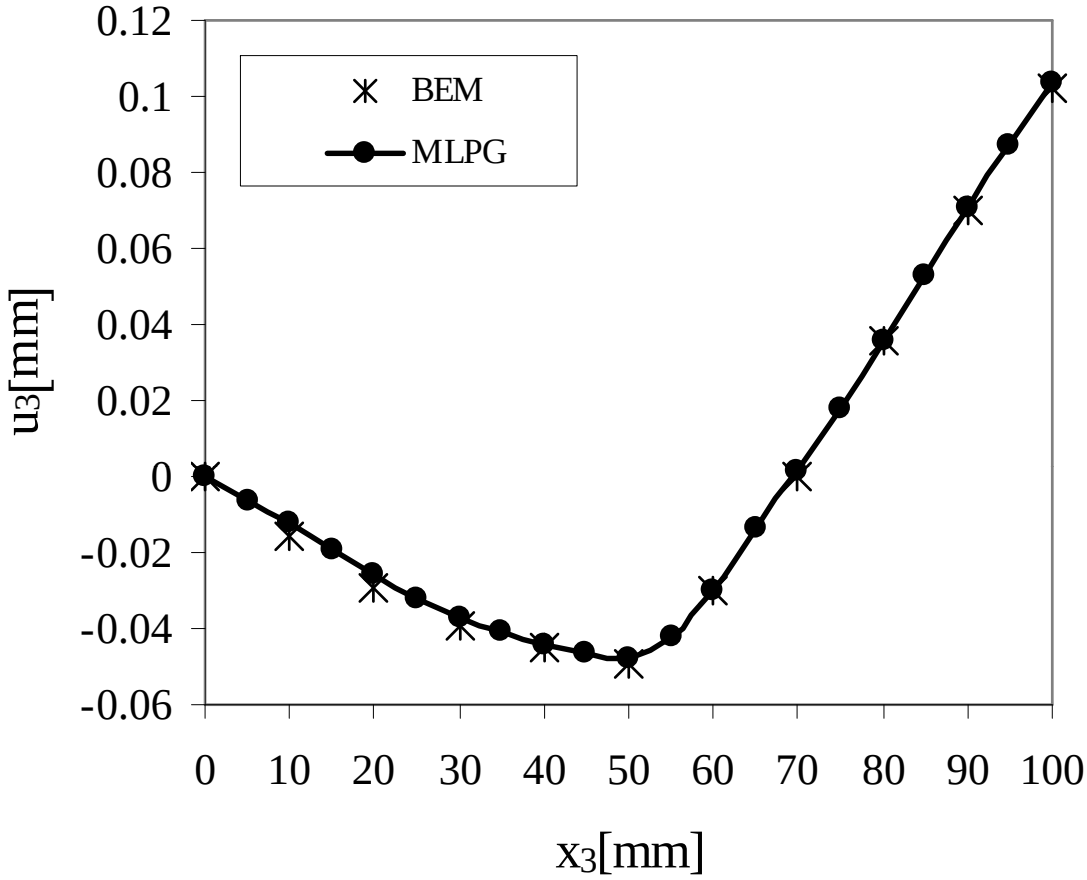

Fig. 4 Variation of the displacement u_3 along x_3-axis at $x_1 = 50mm$ under stationary conditions

Next, transient thermal conditions with Heaviside time variation of a prescribed temperature on the right lateral clamped side are considered.

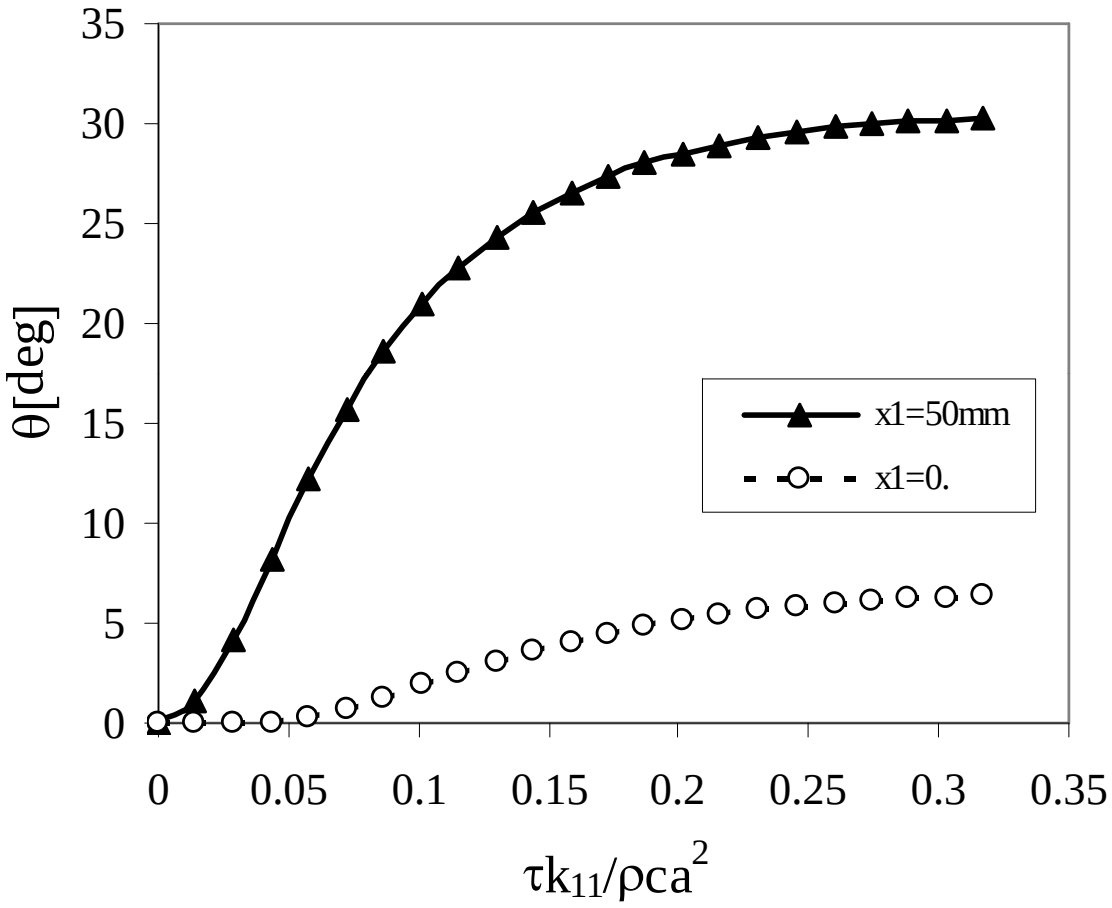

Fig. 5 Time variation of the temperature at nodes A and B

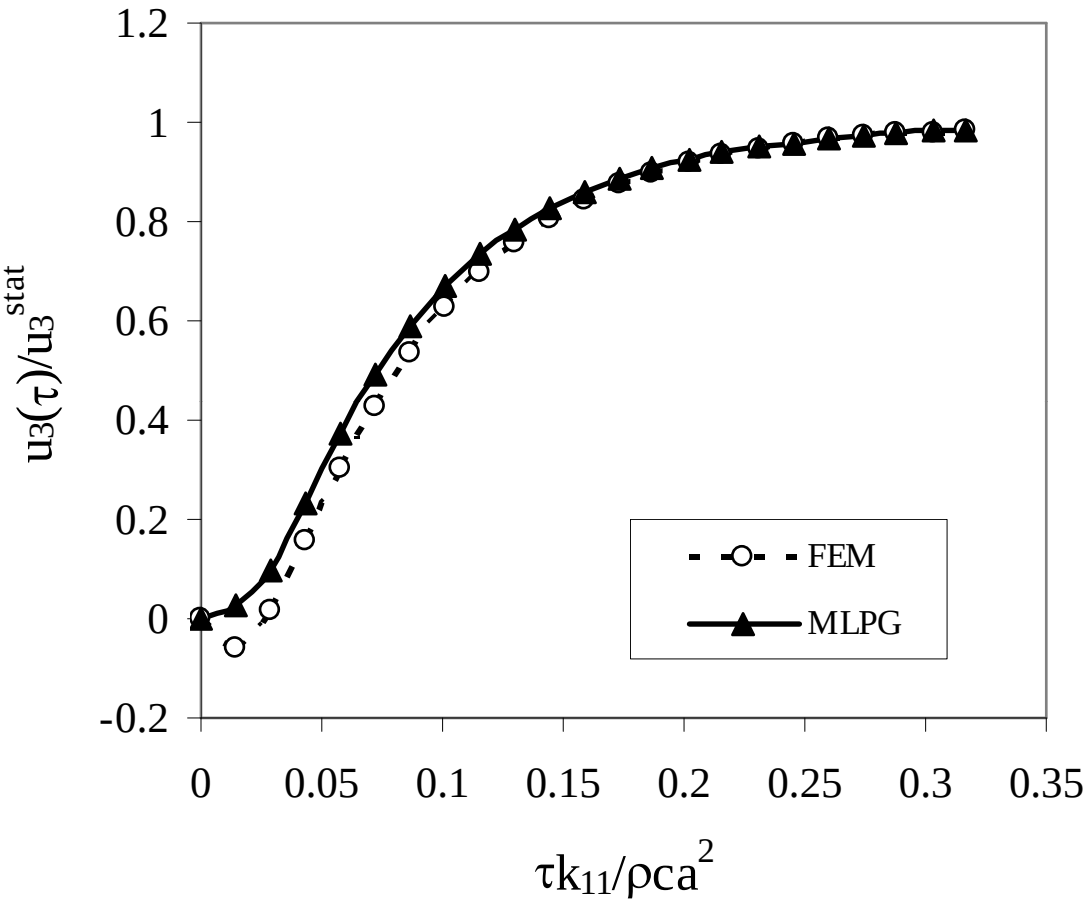

Fig. 6 Time variation of the displacements at node A

A unit square panel under a sudden heating on the top side is analyzed

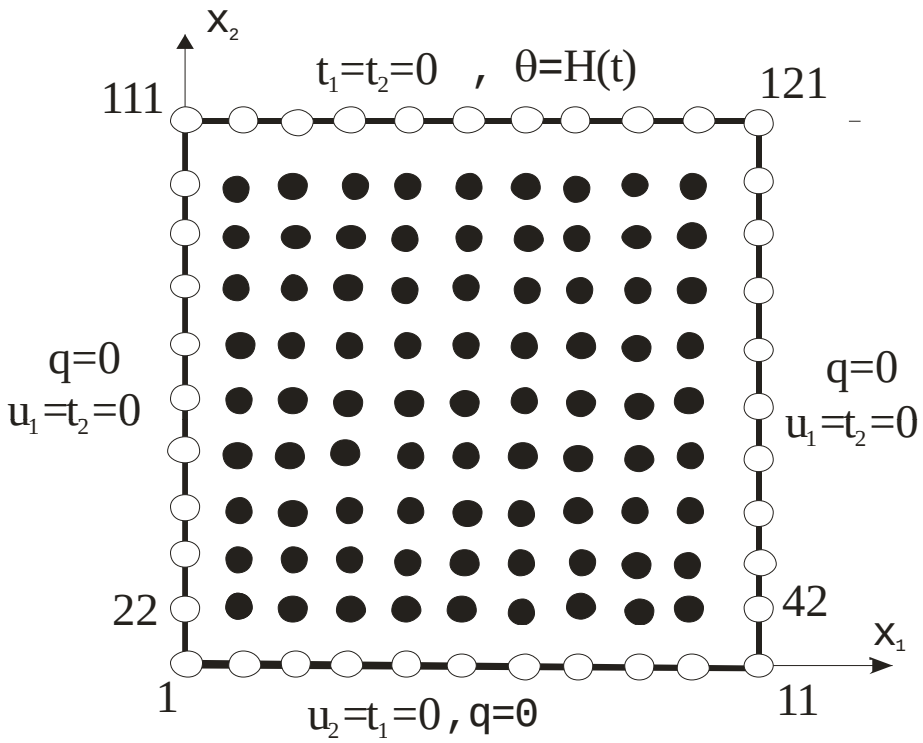

Fig. 7 A suddenly heated unit square panel

The dimensionless thermoelastic coupling parameter

$$\delta = \frac{(1+\nu)\alpha^2 E\theta_0}{(1-\nu)(1-2\nu)\rho c},$$

One can observe that the influence of the mechanical-thermal coupling on both quantities is weaker for small and large time instants.

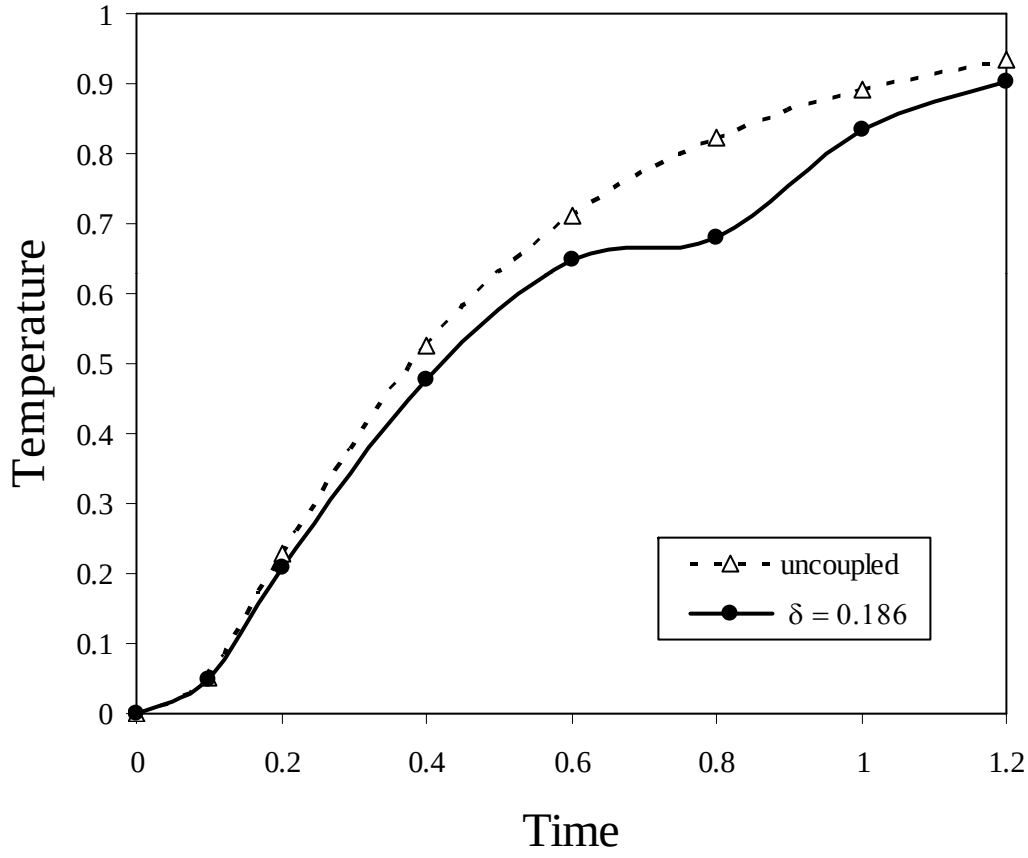

Fig. 8 Coupling effect on the temporal variation of the temperature at $x_2 = 0$

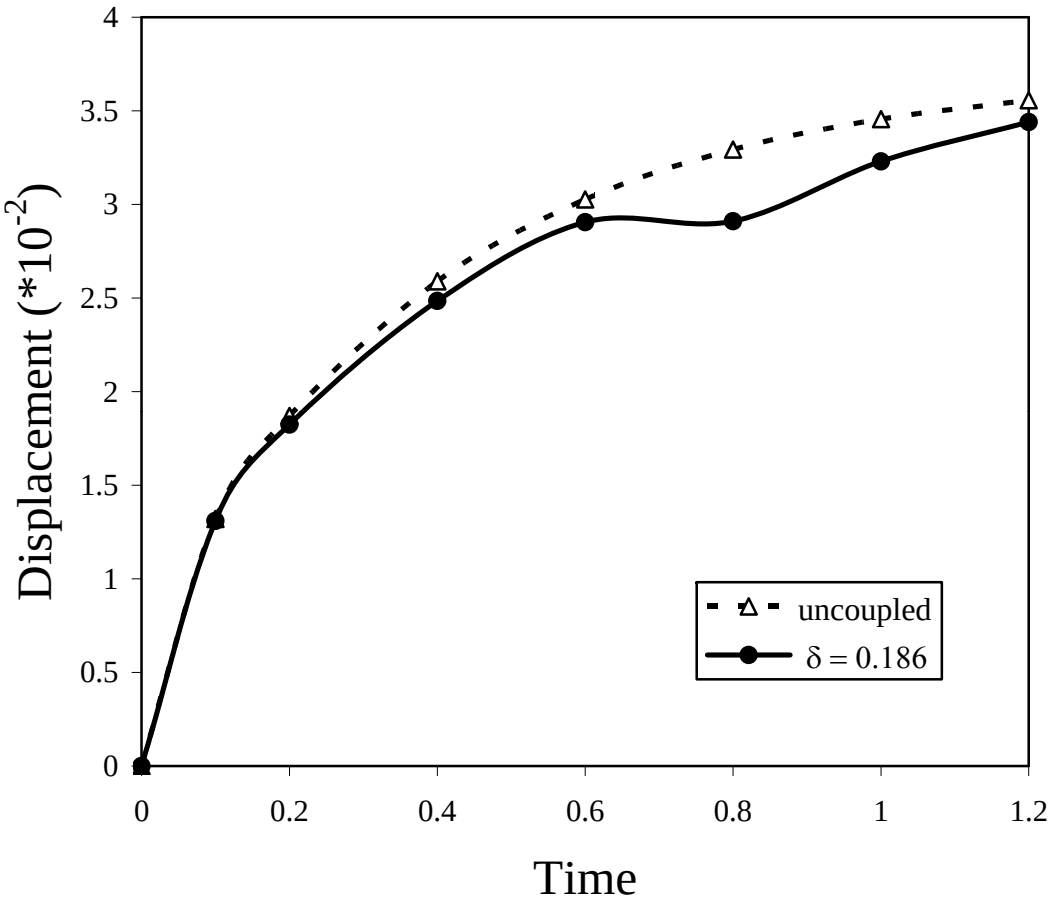

Fig. 9 Coupling effect on the temporal variation of the displacement u_2 at $x_2 = 1$

The LIE method in magneto-electro-thermoelasticity

The magneto-electro-mechanical coupling in some composites can be hundred times higher than in single-phase materials [Nan, (1994); Feng and Su, (2006); Tong et al. (2008)]. Therefore, the multi-field coupling has to be considered in mathematical modeling.

Temperature sensitive, i.e. an electric charge or voltage is generated when temperature variations are exposed - pyroelectric effect.

For typical material coefficients - characteristic frequencies are $f_{th} = 10^{-3}\,\mathrm{Hz}$, $f_{el} = 10^{4}\,\mathrm{Hz}$ and $f_{elm} = 10^{7}\,\mathrm{Hz}$.

Then, the Maxwell equations are reduced to two scalar equations

$$D_{j,j}(\mathbf{x},\tau) = 0, \tag{1}$$

$$B_{j,j}(\mathbf{x},\tau) = 0. \tag{2}$$

The rest of the vectorial Maxwell's equations in quasi-static approximation, $\nabla \times \mathbf{E} = 0$ and $\nabla \times \mathbf{H} = 0$, are satisfied identically by

$$E_j(\mathbf{x},\tau) = -\psi_{,j}(\mathbf{x},\tau)\,, \tag{3}$$

$$H_j(\mathbf{x},\tau) = -\mu_{,j}(\mathbf{x},\tau). \tag{4}$$

The equations of motion and the heat conduction

$$\sigma_{ij,j}(\mathbf{x},\tau) + X_i(\mathbf{x},\tau) = \rho\ddot{u}_i(\mathbf{x},\tau), \tag{5}$$

$$\left[k_{ij}(\mathbf{x})\theta_{,j}(\mathbf{x},\tau)\right]_{,i} - \rho(\mathbf{x})c(\mathbf{x})\dot{\theta}(\mathbf{x},\tau) = 0, \tag{6}$$

Constitutive equations

$$\sigma_{ij}(\mathbf{x},\tau) = c_{ijkl}(\mathbf{x})\varepsilon_{kl}(\mathbf{x},\tau) - e_{kij}(\mathbf{x})E_k(\mathbf{x},\tau) - d_{kij}(\mathbf{x})H_k(\mathbf{x},\tau) - \lambda_{ij}(\mathbf{x})\theta(\mathbf{x},\tau),$$

$$D_j(\mathbf{x},\tau) = e_{jkl}(\mathbf{x})\varepsilon_{kl}(\mathbf{x},\tau) + h_{jk}(\mathbf{x})E_k(\mathbf{x},\tau) + \alpha_{jk}(\mathbf{x})H_k(\mathbf{x},\tau) + p_j(\mathbf{x})\theta(\mathbf{x},\tau),$$

$$B_j(\mathbf{x},\tau) = d_{jkl}(\mathbf{x})\varepsilon_{kl}(\mathbf{x},\tau) + \alpha_{kj}(\mathbf{x})E_k(\mathbf{x},\tau) + \gamma_{jk}(\mathbf{x})H_k(\mathbf{x},\tau) + m_j(\mathbf{x})\theta(\mathbf{x},\tau),$$

$$\begin{bmatrix}\sigma_{11}\\ \sigma_{33}\\ \sigma_{13}\end{bmatrix}=\mathbf{C}(\mathbf{x})\begin{bmatrix}\varepsilon_{11}\\ \varepsilon_{33}\\ 2\varepsilon_{13}\end{bmatrix}-\mathbf{L}(\mathbf{x})\begin{bmatrix}E_1\\ E_3\end{bmatrix}-\mathbf{K}(\mathbf{x})\begin{bmatrix}H_1\\ H_3\end{bmatrix}-\boldsymbol{\lambda}(\mathbf{x})\theta \quad , \tag{12}$$

$$\begin{bmatrix}D_1\\ D_3\end{bmatrix}=\mathbf{G}(\mathbf{x})\begin{bmatrix}\varepsilon_{11}\\ \varepsilon_{33}\\ 2\varepsilon_{13}\end{bmatrix}+\mathbf{H}(\mathbf{x})\begin{bmatrix}E_1\\ E_3\end{bmatrix}+\mathbf{A}(\mathbf{x})\begin{bmatrix}H_1\\ H_3\end{bmatrix}+\boldsymbol{\Pi}(\mathbf{x})\theta, \tag{13}$$

$$\begin{bmatrix}B_1\\ B_3\end{bmatrix}=\mathbf{R}(\mathbf{x})\begin{bmatrix}\varepsilon_{11}\\ \varepsilon_{33}\\ 2\varepsilon_{13}\end{bmatrix}+\mathbf{A}(\mathbf{x})\begin{bmatrix}E_1\\ E_3\end{bmatrix}+\mathbf{F}(\mathbf{x})\begin{bmatrix}H_1\\ H_3\end{bmatrix}+\mathbf{M}(\mathbf{x})\theta, \tag{14}$$

where

$$\boldsymbol{\lambda}=\begin{bmatrix}c_{11} & c_{13} & c_{12}\\ c_{13} & c_{33} & c_{32}\\ 0 & 0 & 0\end{bmatrix}\begin{bmatrix}\beta_{11}\\ \beta_{33}\\ \beta_{22}\end{bmatrix}=\begin{bmatrix}\lambda_{11}\\ \lambda_{33}\\ 0\end{bmatrix}.$$

The following essential and natural boundary conditions are assumed for the mechanical fields

$$u_i(\mathbf{x},\tau) = \tilde{u}_i(\mathbf{x},\tau), \qquad \text{on} \quad \Gamma_u,$$
$$t_i(\mathbf{x},\tau) \equiv \sigma_{ij} n_j = \tilde{t}_i(\mathbf{x},\tau), \qquad \text{on} \quad \Gamma_t, \quad \Gamma = \Gamma_u \cup \Gamma_t.$$

For the electrical fields, we assume

$$\psi(\mathbf{x},\tau) = \tilde{\psi}(\mathbf{x},\tau), \qquad \text{on} \quad \Gamma_p,$$
$$Q(\mathbf{x},\tau) \equiv D_i(\mathbf{x},\tau) n_i(\mathbf{x}) = \tilde{Q}(\mathbf{x},\tau), \qquad \text{on} \quad \Gamma_q, \quad \Gamma = \Gamma_p \cup \Gamma_q,$$

for the magnetic fields

$$\mu(\mathbf{x},\tau) = \tilde{\mu}(\mathbf{x},\tau), \qquad \text{on} \quad \Gamma_a,$$
$$S(\mathbf{x},\tau) \equiv B_i(\mathbf{x},\tau) n_i(\mathbf{x}) = \tilde{S}(\mathbf{x},\tau), \qquad \text{on} \quad \Gamma_b, \quad \Gamma = \Gamma_a \cup \Gamma_b,$$

and for the thermal fields

$$\theta(\mathbf{x},\tau) = \tilde{\theta}(\mathbf{x},\tau) \qquad \text{on} \quad \Gamma_e,$$
$$q(\mathbf{x},\tau) \equiv k_{ij} \theta_{,j}(\mathbf{x},\tau) n_i(\mathbf{x}) = \tilde{q}(\mathbf{x},\tau) \qquad \text{on} \quad \Gamma_f, \quad \Gamma = \Gamma_e \cup \Gamma_f$$

The local weak form of the governing equations (5)

$$\int_{\Omega_s} \left[\sigma_{ij,j}(\mathbf{x},\tau) - \rho \ddot{u}_i(\mathbf{x},\tau) + X_i(\mathbf{x},\tau) \right] u^*_{ik}(\mathbf{x})\, d\Omega = 0 \quad . \tag{15}$$

Applying the Gauss divergence theorem and choosing a Heaviside step function as the test function-the local integral equation

$$\int_{L_s+\Gamma_{su}} t_i(\mathbf{x},\tau) d\Gamma - \int_{\Omega_s} \rho \ddot{u}_i(\mathbf{x},\tau) d\Omega = -\int_{\Gamma_{st}} \tilde{t}_i(\mathbf{x},\tau) d\Gamma - \int_{\Omega_s} X_i(\mathbf{x},\tau) d\Omega \,. \tag{17}$$

The traction components

$$t_i(\mathbf{x},\tau) = \left[c_{ijkl}(\mathbf{x}) u_{k,l}(\mathbf{x},\tau) + e_{kij}(\mathbf{x}) \psi_{,k}(\mathbf{x},\tau) + d_{kij}(\mathbf{x}) \mu_{,k}(\mathbf{x},\tau) - \lambda_{ij}(\mathbf{x}) \theta(\mathbf{x},\tau) \right] n_j(\mathbf{x}) \,.$$

Similarly, the local weak-form of the governing equation (1)

$$\int_{\Omega_s} D_{j,j}(\mathbf{x},\tau) v^*(\mathbf{x})\, d\Omega = 0 \,. \tag{18}$$

Local integral equation

$$\int_{L_s+\Gamma_{sp}} Q(\mathbf{x},\tau)d\Gamma = -\int_{\Gamma_{sq}} \tilde{Q}(\mathbf{x},\tau)d\Gamma, \tag{19}$$

where

$$Q(\mathbf{x},\tau) = D_j(\mathbf{x},\tau)n_j(\mathbf{x}) = \left[e_{jkl}u_{k,l}(\mathbf{x},\tau) - h_{jk}\psi_{,k}(\mathbf{x},\tau) - \alpha_{jk}\mu_{,k}(\mathbf{x},\tau) + p_j\theta(\mathbf{x},\tau) \right] n_j .$$

The LIE corresponding to the governing equation (2)

$$\int_{L_s+\Gamma_{sa}} S(\mathbf{x},\tau)d\Gamma = -\int_{\Gamma_{sb}} \tilde{S}(\mathbf{x},\tau)d\Gamma, \tag{20}$$

where the magnetic flux is given by

$$S(\mathbf{x},\tau) = B_j(\mathbf{x},\tau)n_j(\mathbf{x}) = \left[d_{jkl}u_{k,l}(\mathbf{x},\tau) - \alpha_{kj}\psi_{,k}(\mathbf{x},\tau) - \gamma_{jk}\mu_{,k}(\mathbf{x},\tau) + m_j\theta(\mathbf{x},\tau) \right] n_j .$$

The local weak-form of the diffusion equation (6)

$$\int_{\Omega_s} \left\{ \left[k_{ij}(\mathbf{x})\theta_{,j}(\mathbf{x},\tau) \right]_{,i} - \rho(\mathbf{x})c(\mathbf{x})\dot{\theta}(\mathbf{x},\tau) \right\} w^*(\mathbf{x})\, d\Omega = 0. \tag{21}$$

Local integral equation

$$\int_{L_s+\Gamma_{se}} q(\mathbf{x},\tau)d\Gamma - \int_{\Omega_s} \rho(\mathbf{x})c(\mathbf{x})\dot{\theta}(\mathbf{x},\tau)d\Omega = -\int_{\Gamma_{sf}} \tilde{q}(\mathbf{x},\tau)d\Gamma. \qquad (22)$$

The trial functions in the LIEs are approximated by the Moving Least-Squares (MLS) method

$$\mathbf{u}^h(\mathbf{x},\tau) = \mathbf{\Phi}^T(\mathbf{x})\cdot\hat{\mathbf{u}} = \sum_{a=1}^{n} \phi^a(\mathbf{x})\hat{\mathbf{u}}^a(\tau),$$

$$\psi^h(\mathbf{x},\tau) = \sum_{a=1}^{n} \phi^a(\mathbf{x})\hat{\psi}^a(\tau),$$

$$\mu^h(\mathbf{x},\tau) = \sum_{a=1}^{n} \phi^a(\mathbf{x})\hat{\mu}^a(\tau),$$

$$\theta^h(\mathbf{x},\tau) = \sum_{a=1}^{n} \phi^a(\mathbf{x})\hat{\theta}^a(\tau), \qquad (23)$$

The traction vectors

$$\mathbf{t}^h(\mathbf{x},\tau)=\mathbf{N}(\mathbf{x})\mathbf{C}(\mathbf{x})\sum_{a=1}^{n}\mathbf{B}^a(\mathbf{x})\hat{\mathbf{u}}^a(\tau)\ +\mathbf{N}(\mathbf{x})\mathbf{L}(\mathbf{x})\sum_{a=1}^{n}\mathbf{P}^a(\mathbf{x})\hat{\psi}^a(\tau)+$$

$$+\mathbf{N}(\mathbf{x})\mathbf{K}(\mathbf{x})\sum_{a=1}^{n}\mathbf{P}^a(\mathbf{x})\hat{\mu}^a(\tau)-\mathbf{N}(\mathbf{x})\boldsymbol{\lambda}(\mathbf{x})\sum_{a=1}^{n}\phi^a(\mathbf{x})\hat{\theta}^a(\tau).$$

Electrical charge

$$Q^h(\mathbf{x},\tau)=\mathbf{N}_1(\mathbf{x})\mathbf{G}(\mathbf{x})\sum_{a=1}^{n}\mathbf{B}^a(\mathbf{x})\hat{\mathbf{u}}^a(\tau)-\mathbf{N}_1(\mathbf{x})\mathbf{H}(\mathbf{x})\sum_{a=1}^{n}\mathbf{P}^a(\mathbf{x})\hat{\psi}^a(\tau)-$$

$$-\mathbf{N}_1(\mathbf{x})\mathbf{A}(\mathbf{x})\sum_{a=1}^{n}\mathbf{P}^a(\mathbf{x})\hat{\mu}^a(\tau)+\mathbf{N}_1(\mathbf{x})\boldsymbol{\Pi}(\mathbf{x})\sum_{a=1}^{n}\phi^a(\mathbf{x})\hat{\theta}^a(\tau)$$

Magnetic flux

$$S^h(\mathbf{x},\tau)=\mathbf{N}_1(\mathbf{x})\mathbf{R}(\mathbf{x})\sum_{a=1}^{n}\mathbf{B}^a(\mathbf{x})\hat{\mathbf{u}}^a(\tau)-\mathbf{N}_1(\mathbf{x})\mathbf{A}(\mathbf{x})\sum_{a=1}^{n}\mathbf{P}^a(\mathbf{x})\hat{\psi}^a(\tau)-$$

$$-\mathbf{N}_1(\mathbf{x})\mathbf{F}(\mathbf{x})\sum_{a=1}^{n}\mathbf{P}^a(\mathbf{x})\hat{\mu}^a(\tau)+\mathbf{N}_1(\mathbf{x})\mathbf{M}(\mathbf{x})\sum_{a=1}^{n}\phi^a(\mathbf{x})\hat{\theta}^a(\tau)$$

The heat flux

$$q^h(\mathbf{x},\tau) = k_{ij} n_i \sum_{a=1}^{n} \phi^a_{,j}(\mathbf{x}) \hat{\theta}^a(\tau) = \mathbf{N}_1(\mathbf{x}) \mathbf{\Theta}(\mathbf{x}) \sum_{a=1}^{n} \mathbf{P}^a(\mathbf{x}) \hat{\theta}^a(\tau),$$

The essential boundary conditions

$$\sum_{a=1}^{n} \phi^a(\zeta) \hat{\mathbf{u}}^a(\tau) = \tilde{\mathbf{u}}(\zeta,\tau) \quad \text{for} \quad \zeta \in \Gamma_u,$$

$$\sum_{a=1}^{n} \phi^a(\zeta) \hat{\psi}^a(\tau) = \tilde{\psi}(\zeta,\tau) \quad \text{for} \quad \zeta \in \Gamma_p,$$

$$\sum_{a=1}^{n} \phi^a(\zeta) \hat{\mu}^a(\tau) = \tilde{\mu}(\zeta,\tau) \quad \text{for} \quad \zeta \in \Gamma_a,$$

$$\sum_{a=1}^{n} \phi^a(\zeta) \hat{\theta}^a(\tau) = \tilde{\theta}(\zeta,\tau) \quad \text{for} \quad \zeta \in \Gamma_e.$$

Discretized forms of LIE

$$\sum_{a=1}^{n}\left[\left(\int_{L_s+\Gamma_{st}}\mathbf{N}(\mathbf{x})\mathbf{C}(\mathbf{x})\mathbf{B}^a(\mathbf{x})d\Gamma\right)\hat{\mathbf{u}}^a(\tau)-\left(\int_{\Omega_s}\rho(\mathbf{x})\phi^a d\Omega\right)\ddot{\hat{\mathbf{u}}}^a(\tau)\right]+$$

$$+\sum_{a=1}^{n}\left(\int_{L_s+\Gamma_{st}}\mathbf{N}(\mathbf{x})\mathbf{L}(\mathbf{x})\mathbf{P}^a(\mathbf{x})d\Gamma\right)\hat{\boldsymbol{\psi}}^a(\tau)+\sum_{a=1}^{n}\left(\int_{L_s+\Gamma_{st}}\mathbf{N}(\mathbf{x})\mathbf{K}(\mathbf{x})\mathbf{P}^a(\mathbf{x})d\Gamma\right)\hat{\boldsymbol{\mu}}^a(\tau)-$$

$$-\sum_{a=1}^{n}\left(\int_{L_s+\Gamma_{st}}\mathbf{N}(\mathbf{x})\boldsymbol{\lambda}(\mathbf{x})\phi^a(\mathbf{x})d\Gamma\right)\hat{\theta}^a(\tau)=-\int_{\Gamma_{st}}\tilde{\mathbf{t}}(\mathbf{x},\tau)d\Gamma-\int_{\Omega_s}\mathbf{X}(\mathbf{x},\tau)d\Omega,$$

$$\sum_{a=1}^{n}\left(\int_{L_s+\Gamma_{sq}}\mathbf{N}_1(\mathbf{x})\mathbf{G}(\mathbf{x})\mathbf{B}^a(\mathbf{x})d\Gamma\right)\hat{\mathbf{u}}^a(\tau)-\sum_{a=1}^{n}\left(\int_{L_s+\Gamma_{sq}}\mathbf{N}_1(\mathbf{x})\mathbf{H}(\mathbf{x})\mathbf{P}^a(\mathbf{x})d\Gamma\right)\hat{\boldsymbol{\psi}}^a(\tau)-$$

$$-\sum_{a=1}^{n}\left(\int_{L_s+\Gamma_{sq}}\mathbf{N}_1(\mathbf{x})\mathbf{A}(\mathbf{x})\mathbf{P}^a(\mathbf{x})d\Gamma\right)\hat{\boldsymbol{\mu}}^a(\tau)+\sum_{a=1}^{n}\left(\int_{L_s+\Gamma_{sq}}\mathbf{N}_1(\mathbf{x})\boldsymbol{\Pi}(\mathbf{x})\phi^a(\mathbf{x})d\Gamma\right)\hat{\theta}^a(\tau)=$$

$$=-\int_{\Gamma_{sq}}\tilde{Q}(\mathbf{x},\tau)d\Gamma,$$

$$\sum_{a=1}^{n}\left(\int_{L_s+\Gamma_{sb}}\mathbf{N}_1(\mathbf{x})\mathbf{R}(\mathbf{x})\mathbf{B}^a(\mathbf{x})d\Gamma\right)\hat{\mathbf{u}}^a(\tau)\ -\sum_{a=1}^{n}\left(\int_{L_s+\Gamma_{sb}}\mathbf{N}_1(\mathbf{x})\mathbf{A}(\mathbf{x})\mathbf{P}^a(\mathbf{x})d\Gamma\right)\hat{\boldsymbol{\psi}}^a(\tau)-$$

$$-\sum_{a=1}^{n}\left(\int_{L_s+\Gamma_{sb}}\mathbf{N}_1(\mathbf{x})\mathbf{F}(\mathbf{x})\mathbf{P}^a(\mathbf{x})d\Gamma\right)\hat{\boldsymbol{\mu}}^a(\tau)+\sum_{a=1}^{n}\left(\int_{L_s+\Gamma_{sb}}\mathbf{N}_1(\mathbf{x})\mathbf{M}(\mathbf{x})\phi^a(\mathbf{x})d\Gamma\right)\hat{\theta}^a(\tau)=$$

$$=-\int_{\Gamma_{sb}}\tilde{S}(\mathbf{x},\tau)d\Gamma,$$

$$\sum_{a=1}^{n}\left[\left(\int_{L_s+\Gamma_{sf}}\mathbf{N}_1(\mathbf{x})\boldsymbol{\Theta}(\mathbf{x})\mathbf{P}^a(\mathbf{x})d\Gamma\right)\hat{\theta}^a(\tau)-\left(\int_{\Omega_s}\rho c\phi^a(\mathbf{x})d\Gamma\right)\dot{\hat{\theta}}^a(\tau)\right]\ =$$

$$=-\int_{\Gamma_{sf}}\tilde{q}(\mathbf{x},\tau)d\Gamma\ .$$

Collecting the discretized LIEs together with the discretized boundary conditions - matrix form the system becomes

$$\mathbf{A}\ddot{\mathbf{x}} + \mathbf{B}\dot{\mathbf{x}} + \mathbf{C}\mathbf{x} = \mathbf{Y} \quad .$$

The Houbolt method is applied

$$\ddot{\mathbf{x}}_{\tau+\Delta\tau} = \frac{2\mathbf{x}_{\tau+\Delta\tau} - 5\mathbf{x}_{\tau} + 4\mathbf{x}_{\tau-\Delta\tau} - \mathbf{x}_{\tau-2\Delta\tau}}{\Delta\tau^2}$$

The backward difference method for "velocities"

$$\dot{\mathbf{x}}_{\tau+\Delta\tau} = \frac{\mathbf{x}_{\tau+\Delta\tau} - \mathbf{x}_{\tau}}{\Delta\tau} \quad .$$

System of algebraic equations for the unknowns

$$\left[\frac{2}{\Delta\tau^2}\mathbf{A} + \frac{1}{\Delta\tau}\mathbf{B} + \mathbf{C}\right]\mathbf{x}_{\tau+\Delta\tau} = \frac{1}{\Delta\tau^2}(5\mathbf{A} + \mathbf{B}\Delta\tau)\mathbf{x}_{\tau} + \mathbf{A}\frac{1}{\Delta\tau^2}\left\{-4\mathbf{x}_{\tau-\Delta\tau} + \mathbf{x}_{\tau-2\Delta\tau}\right\} +$$

Numerical examples

3.1 A central crack in a finite homogeneous strip

On the outer boundary of the strip a thermal load $T_2 = \theta_0 = 1\text{deg}$

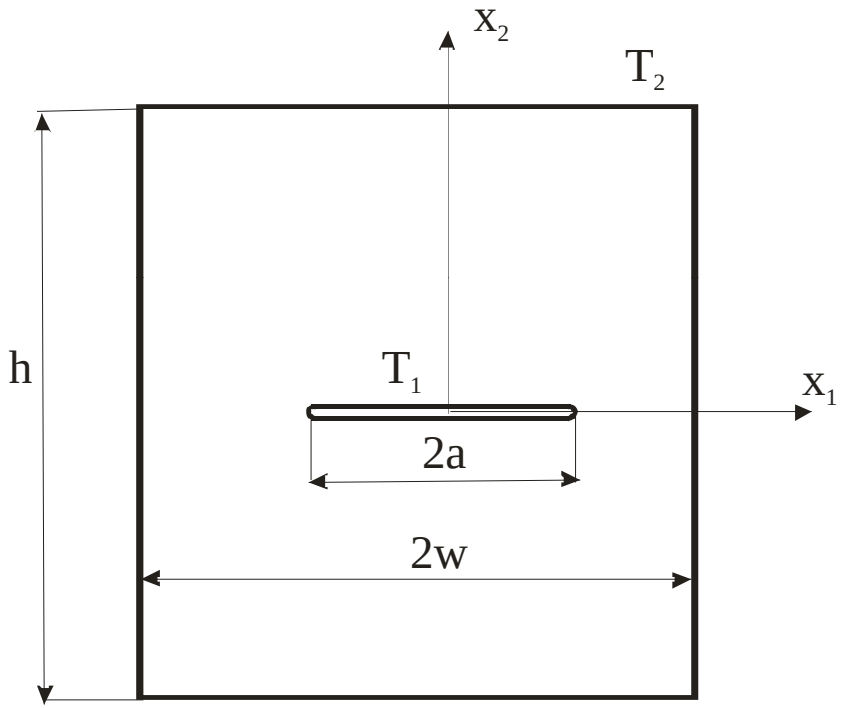

Fig.1 Central crack in a finite strip with prescribed temperatures on outer boundary and crack surfaces

930 (31x30) nodes

The material coefficients for the $BaTiO_3$-$CoFe_2O_4$ composite

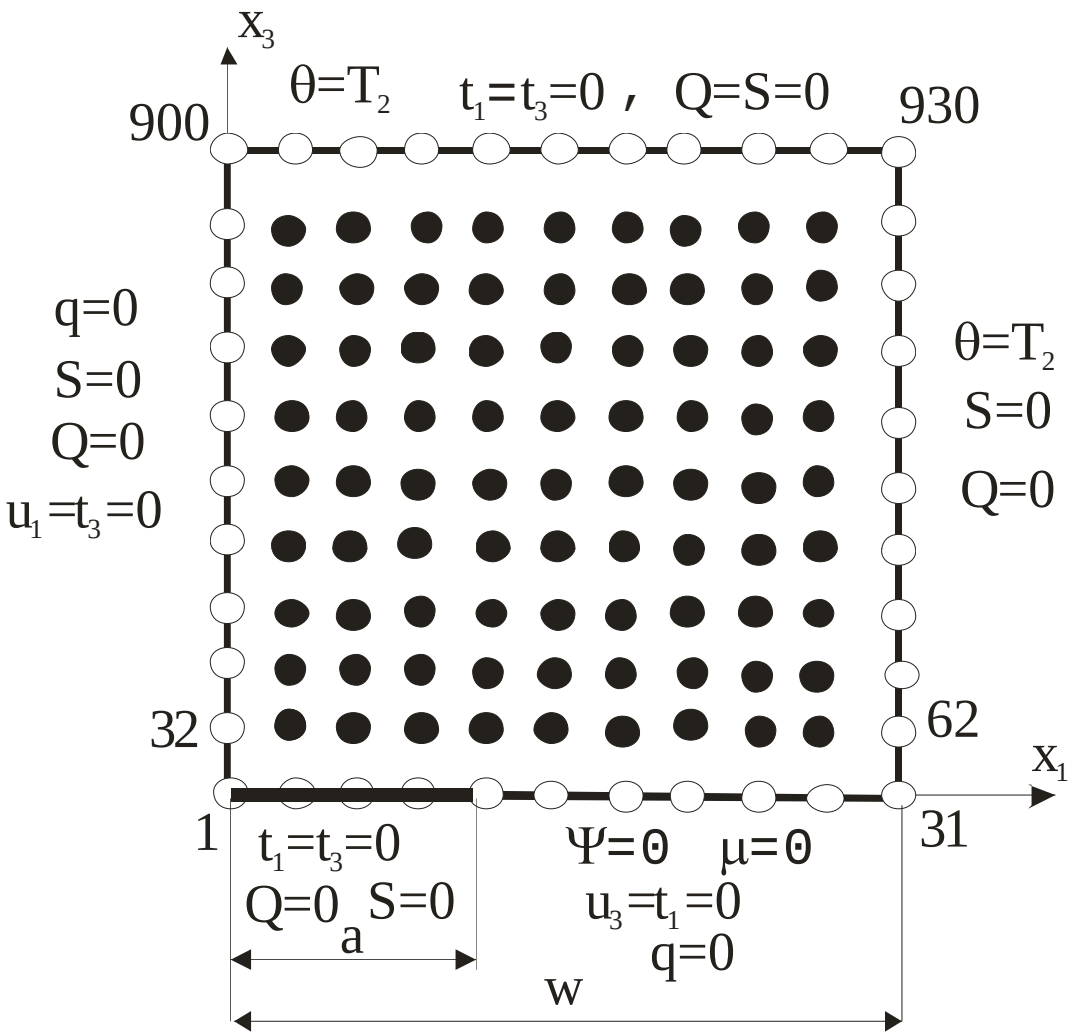

Fig. 2 Node distribution and boundary conditions

The considered finite values of the pyroelectric and pyromagnetic parameters reduce the crack-opening-displacements.

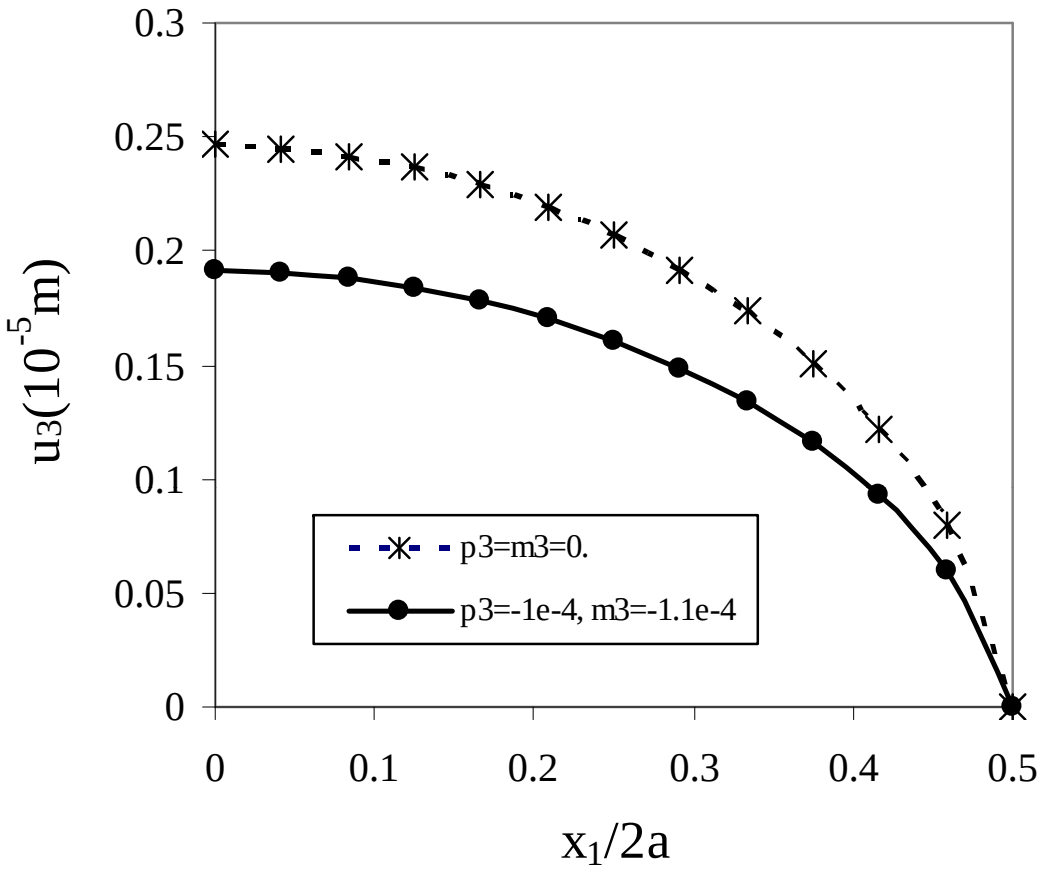

Fig. 3 Variations of the crack-opening-displacement with the normalized coordinate $x_1 / 2a$

Oppositely, the electrical potential is significantly increased if finite values of pyroelectric and pyromagnetic parameters are considered

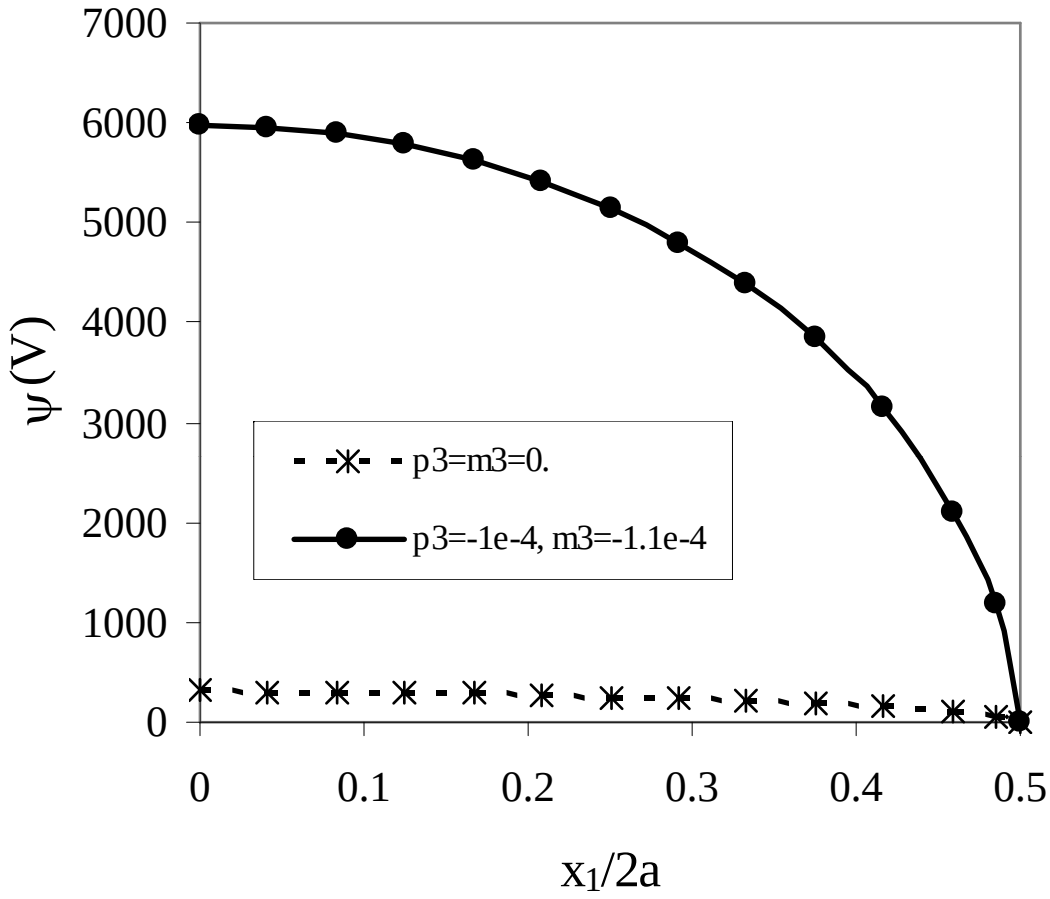

Fig. 4 Variations of the electrical potential along the crack face

The magnetic potential is slightly reduced for finite values of the pyroelectric and pyromagnetic parameters (Fig. 5).

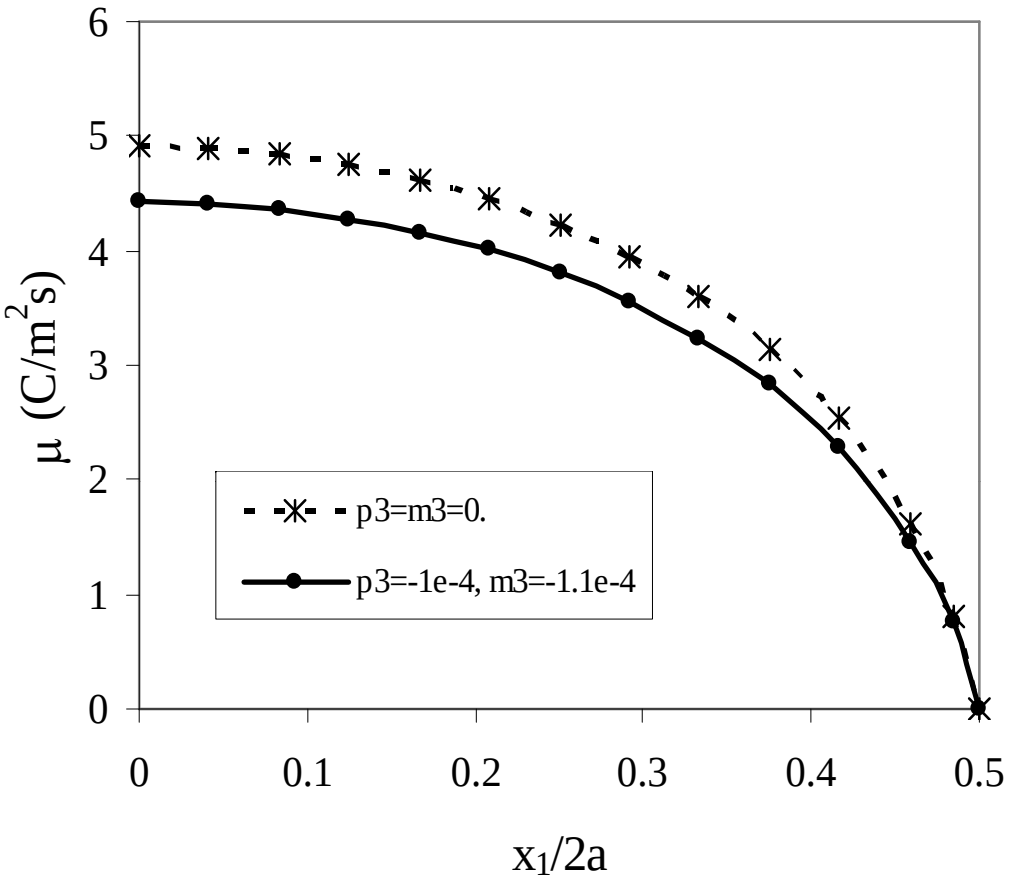

Fig. 5 Variations of the magnetic potential along the crack face

In the crack tip vicinity, the displacements and potentials show the classical $\sqrt{r}$ asymptotic behavior. Generalized intensity factors

$$\begin{pmatrix} K_{II} \\ K_I \\ K_E \\ K_M \end{pmatrix} = \sqrt{\frac{\pi}{2r}} \left[\mathrm{Re}(\mathbf{B})^{-1} \right] \begin{pmatrix} u_1 \\ u_3 \\ \psi \\ \mu \end{pmatrix} ,$$

where the matrix **B** is determined by the material properties and

$$K_I = \lim_{r \to 0} \sqrt{2\pi r}\, \sigma_{33}(r,0),$$

$$K_{II} = \lim_{r \to 0} \sqrt{2\pi r}\, \sigma_{13}(r,0),$$

$$K_E = \lim_{r \to 0} \sqrt{2\pi r}\, D_3(r,0),$$

$$K_M = \lim_{r \to 0} \sqrt{2\pi r}\, B_3(r,0).$$

The finite values of pyroelectric and pyromagnetic parameters have vanishing influence on the stress intensity factor and its value is $K_I = 4.48 \cdot 10^5 \,\mathrm{Pa} \cdot \mathrm{m}^{1/2}$.

The electrical and magnetic potentials ψ , μ on crack surfaces do not result in a finite value of the EDIF, K_E and the MIIF, K_M .
It means that the crack-opening-displacement u_3 and the potentials ψ , μ are coupled, but the SIF , and the EDIF and MIIF in this case are uncoupled.

3.2 Edge crack in a finite strip under a thermal shock

On the left lateral side of the strip a cooling shock with Heaviside time variation is applied. The right lateral side is kept at vanishing temperature. The material properties $BaTiO_3$-$CoFe_2O_4$.

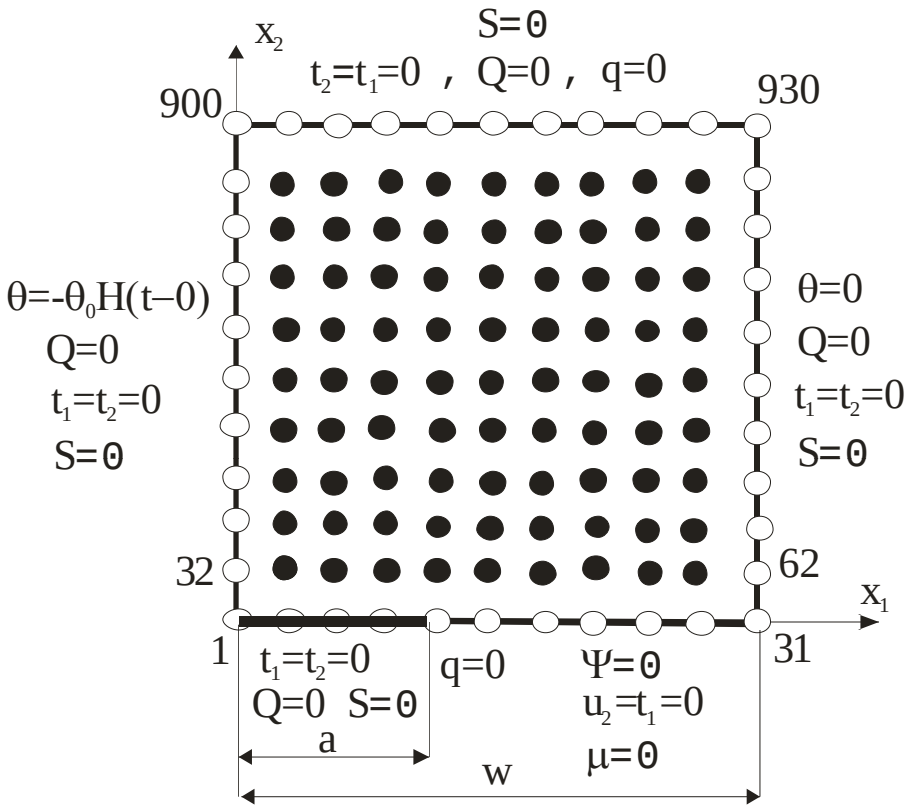

Fig. 6 Edge crack in a finite strip under a thermal shock on the lateral side

The electromagnetic and piezomagnetic parameters have only small influence on the displacement and electrical potential.

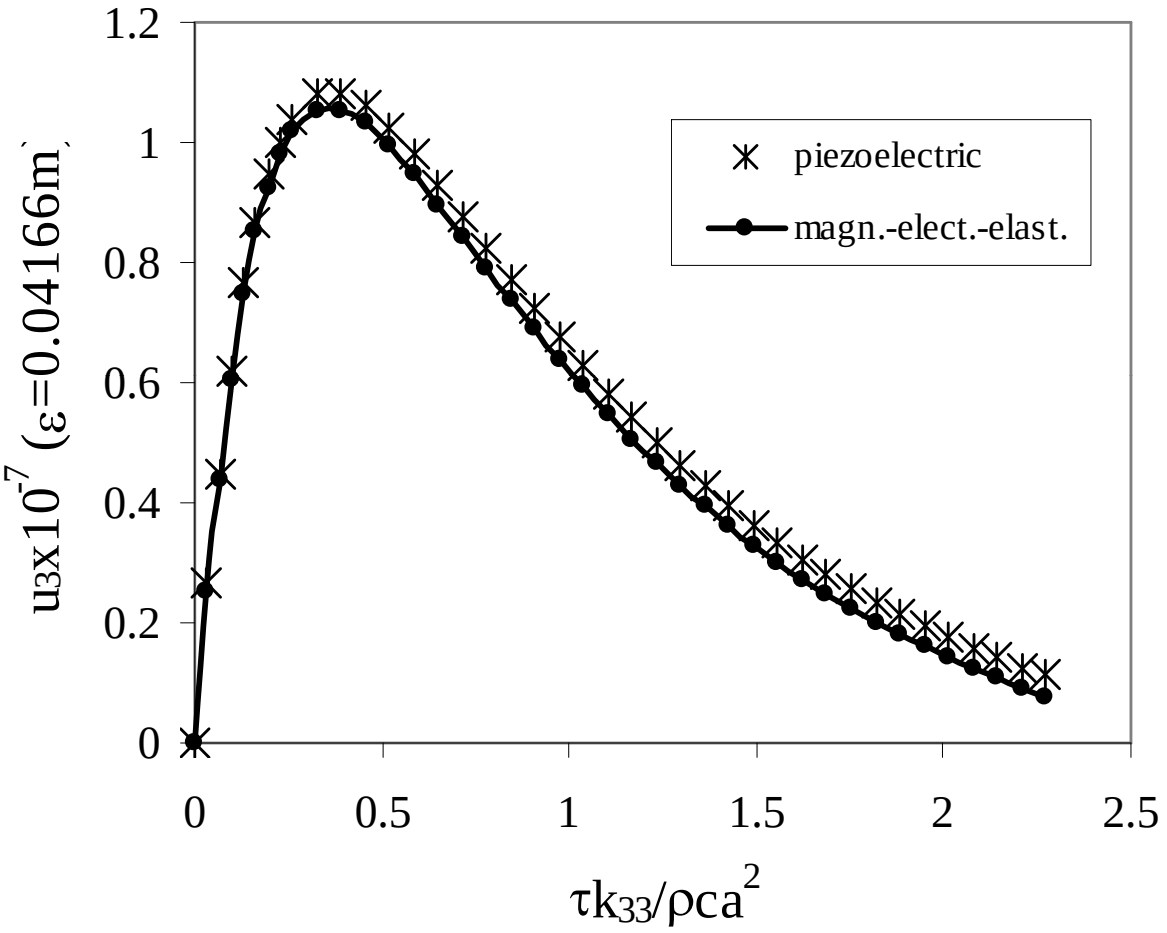

Fig. 7 Time evolution of the crack displacement at the crack-tip vicinity

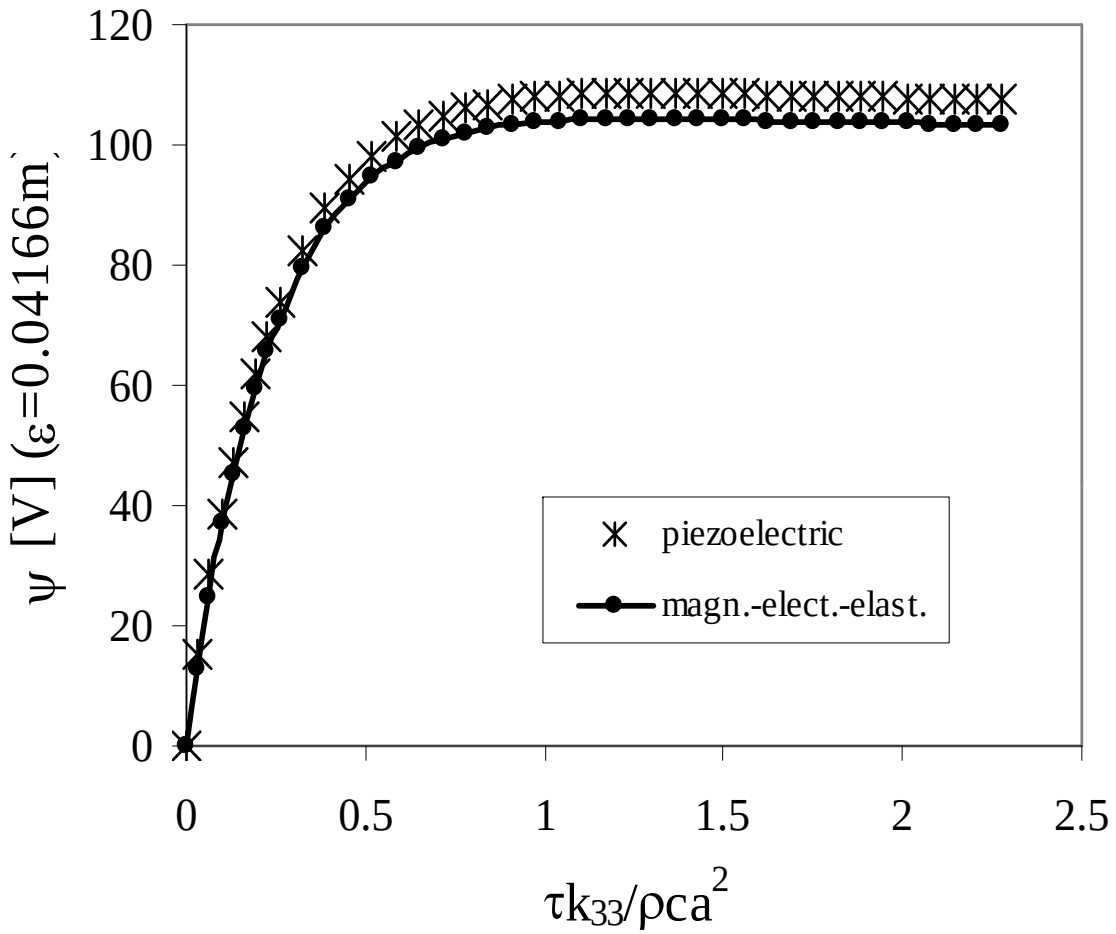

Fig. 8 Time evolution of the electrical potential at the crack-tip vicinity

Variations of the displacement, electrical and magnetic potentials along the crack face at the time instant $\tau^* = 0.909$ are presented in Fig. 9.

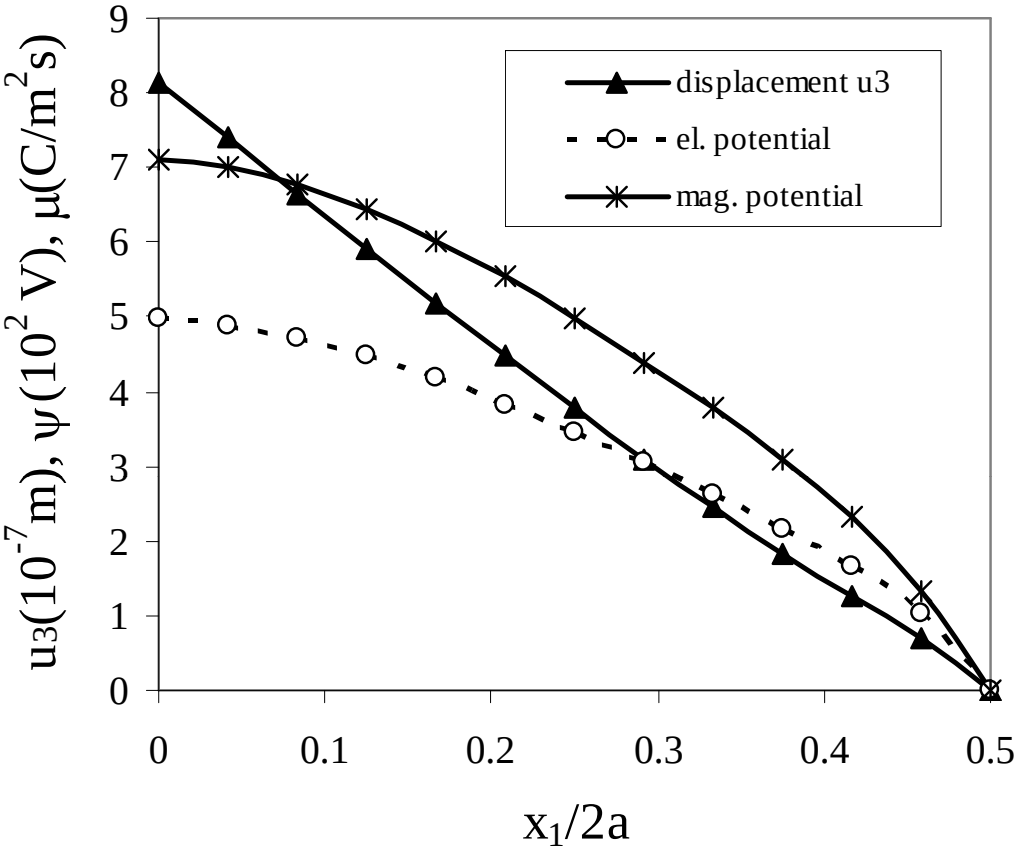

Fig. 9 Variations of the displacement, electrical and magnetic potentials along the crack face at $\tau^* = 0.909$

One can observe that the gradient of the crack-opening- displacement along x_1 is significantly larger than in the previous central crack problem.

Numerical results for the normalized SIF $f_I = K_I / \left(\sqrt{\pi a}\, \beta_{11} c_{11} \theta_0 \right)$

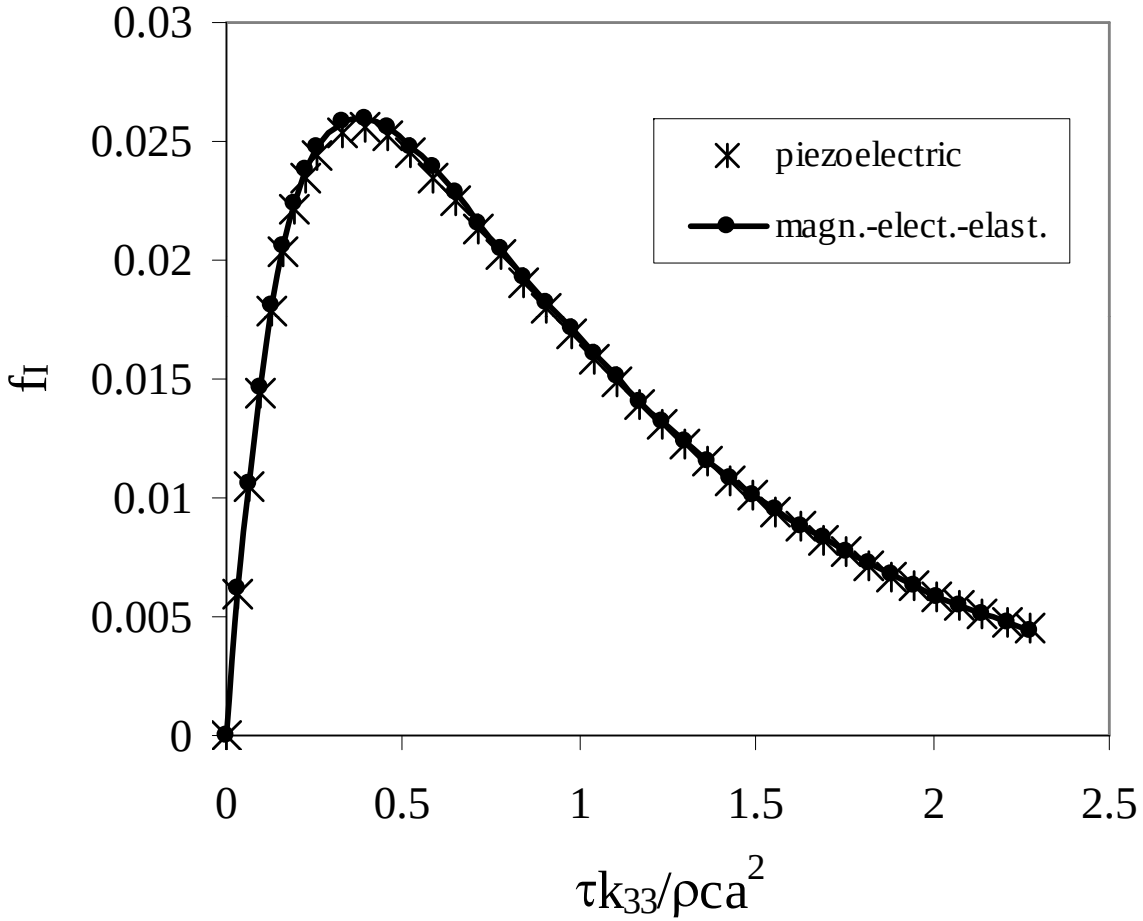

Fig. 10 Time evolution of the normalized SIF in the cracked strip under a thermal shock

The normalized EDIF is defined as $f_{IV} = \Lambda K_E / \left(\sqrt{\pi a}\, \beta_{11} c_{11} \theta_0 \right)$, where $\Lambda = e_{33} / h_{33}$.

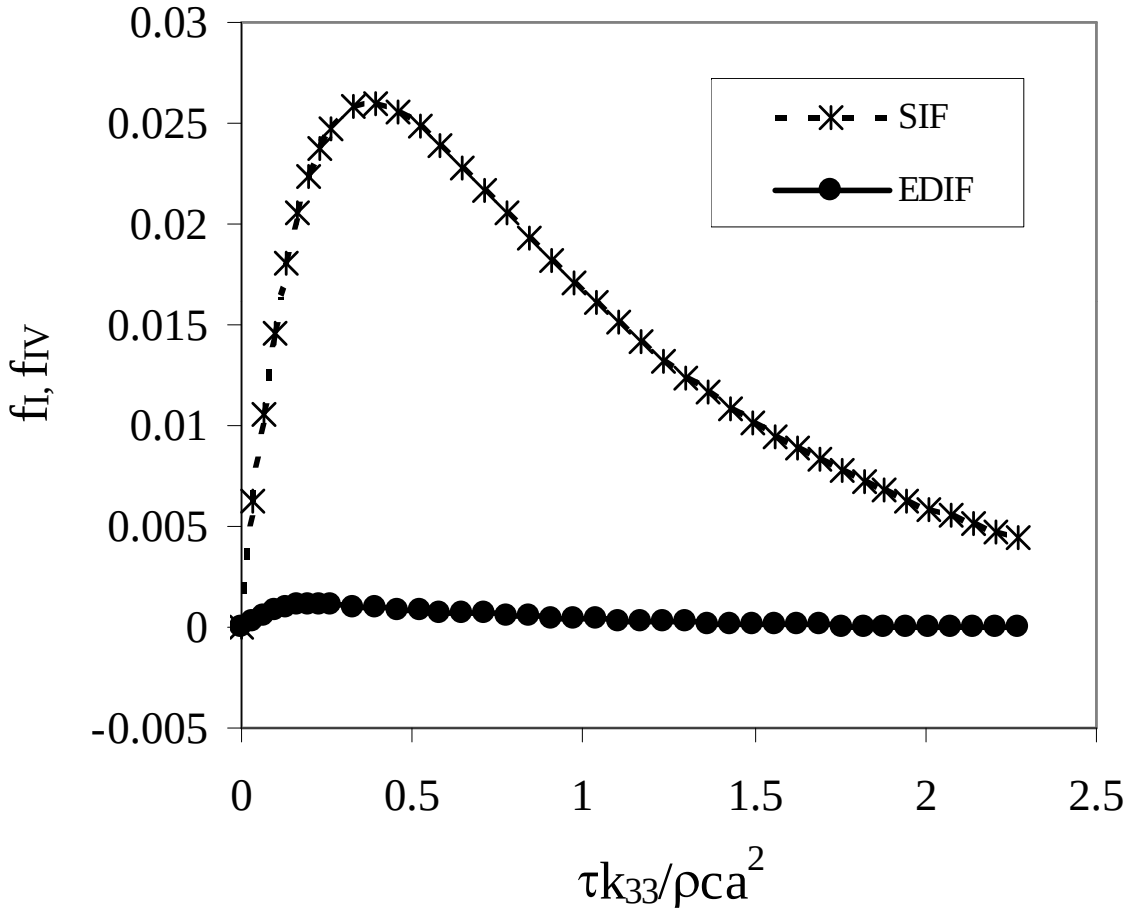

Fig. 11 Comparison of the normalized SIF and EDIF in the cracked strip under a thermal shock

An exponential variation

$$f_{ij}(\mathbf{x}) = f_{ij0}\exp(\gamma_f x_1).$$

$\gamma = 1$ except the heat conduction and linear thermal expansion coefficients where $\gamma = -1$. Pyroelectric and pyromagnetic coefficients are assumed to be zero.

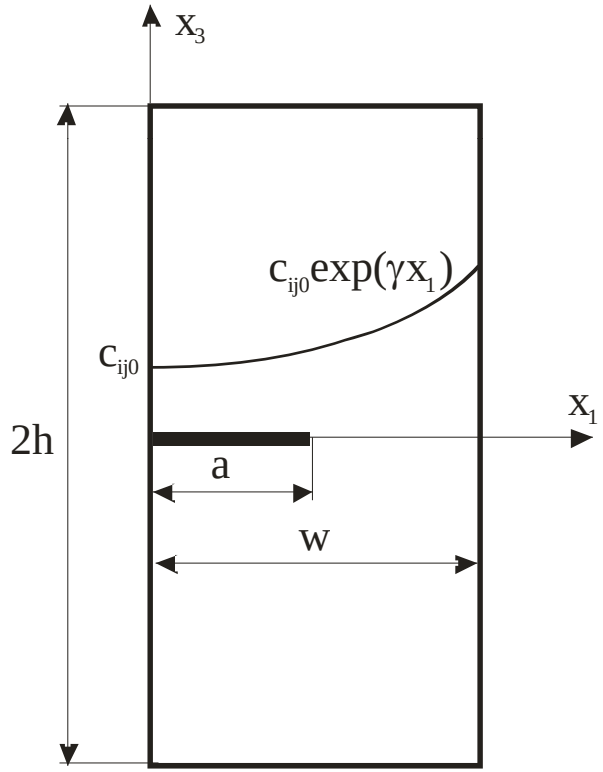

Fig. 12 An edge crack in a finite strip with graded material properties in x_1

From the numerical analyses it follows that COD and potential values are similar in the real homogeneous and FGM

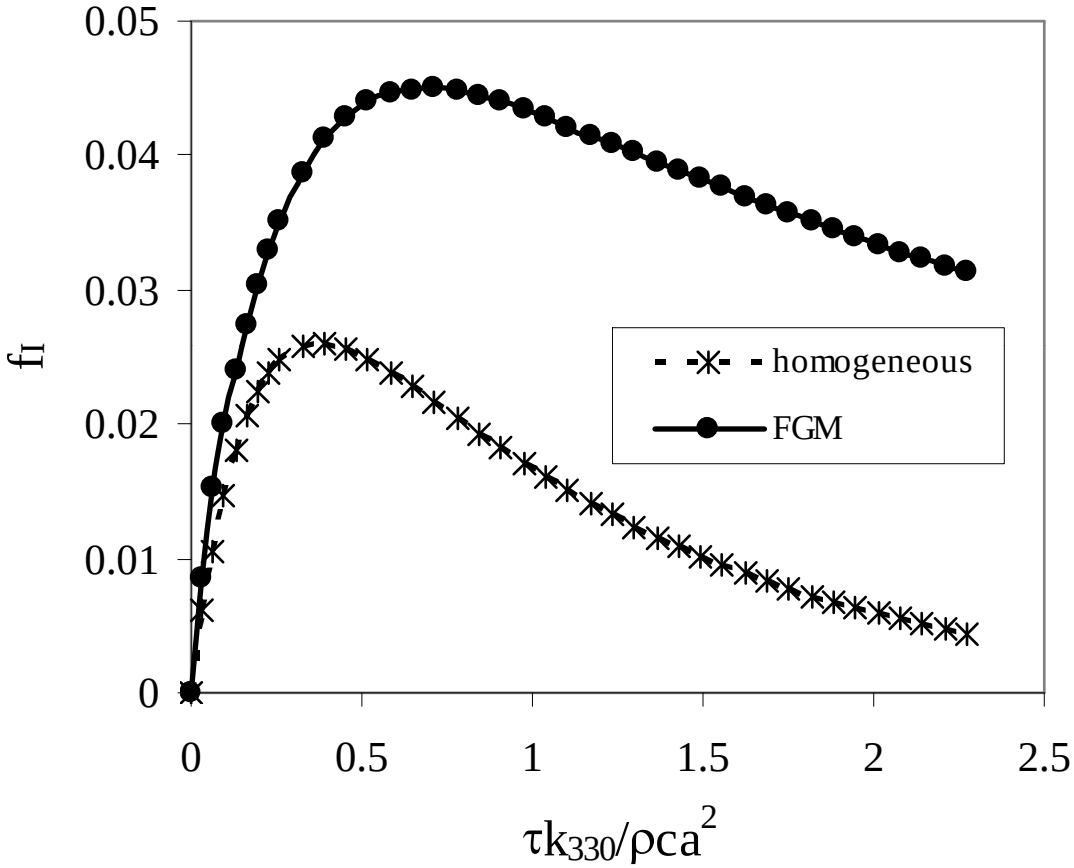

Fig. 13 Time evolution of the SIF in the cracked FGM strip under a thermal shock

thermal conductivity in FGM is smaller than in the homog. case

Conclusions

- A meshless local integral equation method is proposed for solution of boundary value problems for coupled thermoelasticity, and magneto-electro-thermoelasticity. Transient dynamic governing equations are considered here.
- 2-D and 3-D problems
- Inertial and diffusive terms are approximated by Houbolt finite-difference scheme and backward finite difference, respectively
- Material properties can be considered as continuously nonhomogeneous.
- The analyzed domain is divided into small overlapping circular or spherical subdomains. The Moving Least-Squares (MLS) scheme is adopted for the approximation of the physical field quantities.
- The main advantage of the present method is its simplicity and generality.